A self scale Z-pinch
Scalability, Similarities and Differences in Plasma Focus Devices:
Diagnostics
Basic Research and Applications

Part 2

Leopoldo Soto

Comisión Chilena de Energía Nuclear (CCHEN)
Center for Research and Aplications in Plasma Physics and Pulsed Power, P4
Santiago, Chile

LEOPOLDO.SOTO@CCHEN.CL

Topics

Part 1. Basic concepts. Z-pinch, pulsed power, plasma focus.

Part 2. How to obtain information from a dense transient plasma? Plasma diagnostics

Basic Research and Applications

Part 3. How to design and to build a small plasma focus? Tricks and Recipes

Part 2: outline

- How to obtain information from a dense transient plasma?
  Plasma diagnostics
- Basic research:
  - Plasma dynamics, singularities structures, filaments, schoks, jets
- Applications:
  - As x-rays and neutron sources
  - To study materials for fusion reactors
  - Film deposition
  - To study the effects of puldsed radiation on life matter
  - Plasma thrusters for nanosatellites

How to obtain information from a dense transient plasma

Diagnostics

- **Electrical signals**
- **Visible plasma images**
- **X-ray detections (temporal and spatial resolution)**
- **Neutron detection (in particular low yield pulses)**
- **Charged particles**
- **Optical refractive diagnostics**
- **Spectroscopy**

Electrical signals

$$V_2 = \frac{R_2}{R_1 + R_2} V_1$$

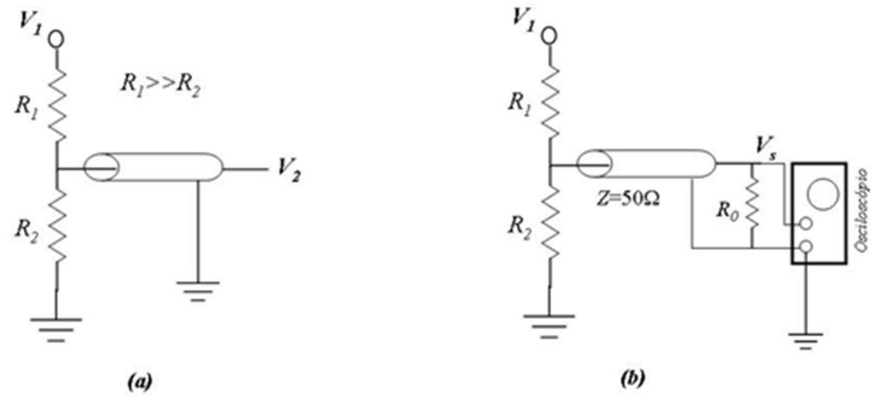

Voltage monitor: resistive divider

$$V \alpha \ dI/dt$$

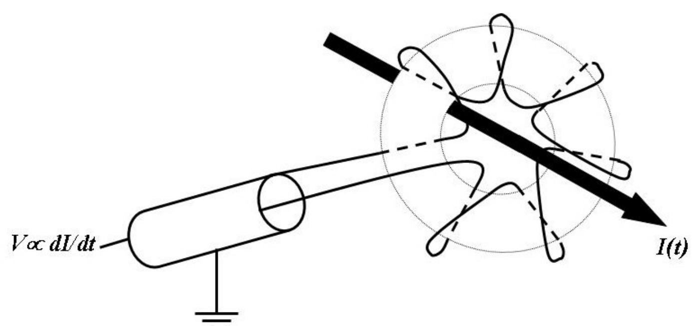

Current monitor: Rogowski coil

Electrical signals

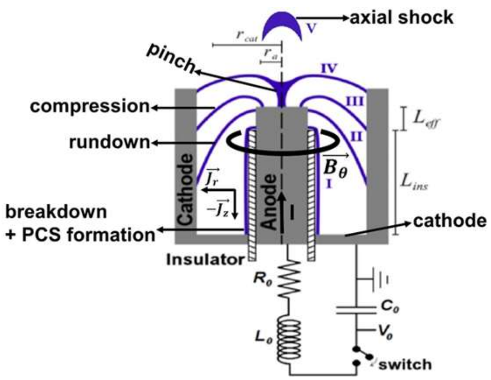

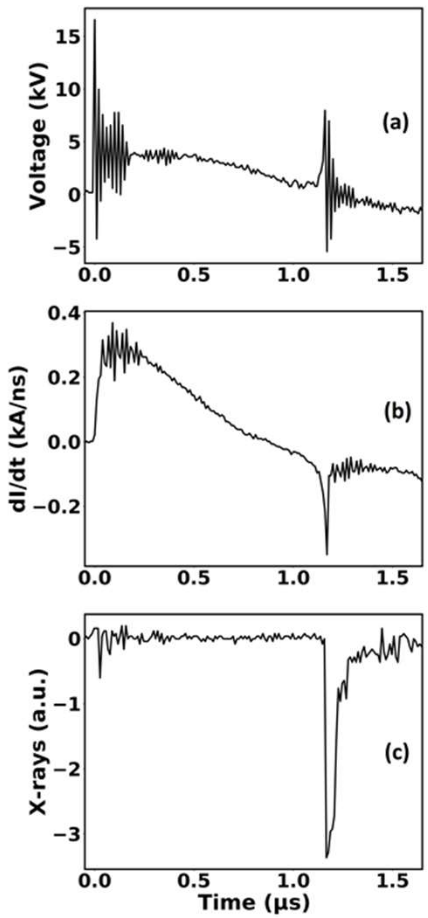

$$V(t) = \frac{d}{dt}[(L_p(t) + L_0)I(t)] \qquad (1)$$

That gives

$$L_p(t) = \frac{\int_{to}^{t} V(t)dt + (L_0 + L_p(t_0))I(t_0)}{I(t)} - L_0$$

or

$$L_p(t) + L_0 = \frac{\int_{to}^{t} V(t)dt + (L_0 + L_p(t_0))I(t_0)}{I(t)} \qquad (2)$$

$$L_P(t) = L_P(t_c) + L'_P(t) \qquad (4)$$

for $t > t_c$:

$$V(t) = [L_0 + L_P(t_c)]\frac{dI}{dt} + \frac{d}{dt}(IL'_P) \qquad (5)$$

$$V_P = V(t) - (L_0 + L_P(t_c))\frac{dI}{dt} \qquad (6)$$

with

$$V_P = \frac{d(IL'_P)}{dt} \qquad (7)$$

F. Veloso, C. Pavez, J. Moreno, V. Galaz, M. Zambra and L. Soto, Journal of Fusion Energy **31**, 30-37 (2012)

Electrical signals

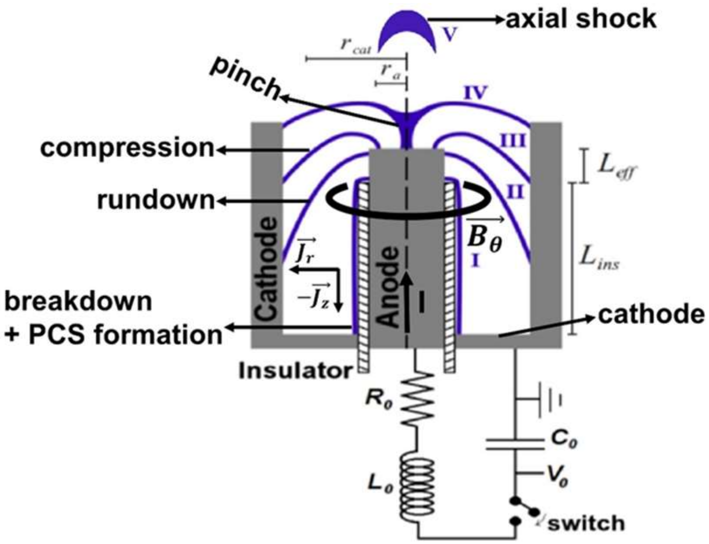

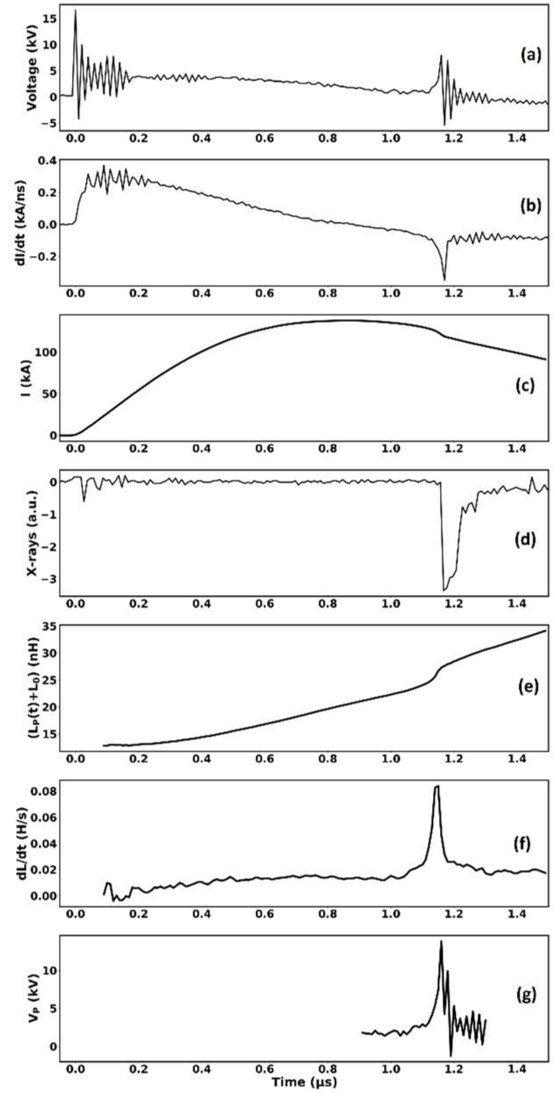

$$L_p(t) = (\mu_0 / 2\pi)\, z(t) \ln(b/r(t))$$

Visible plasma images

Images from plasma light are captured with a ICCD camera, 4ns exposure time

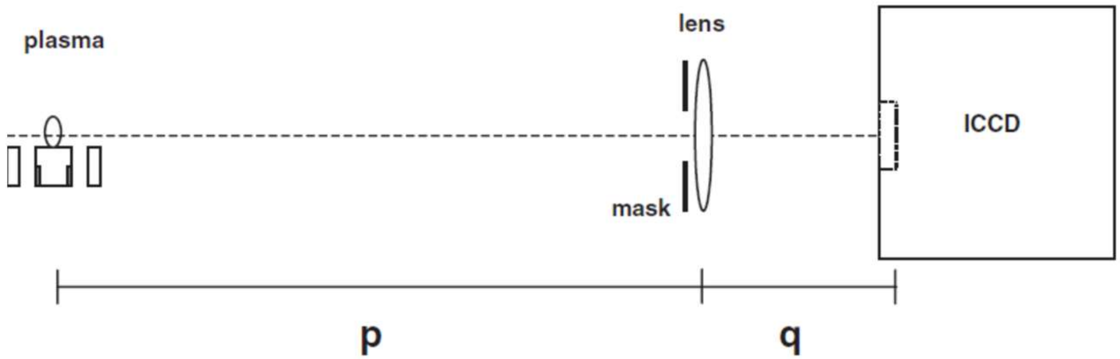

- Plasma Dynamics

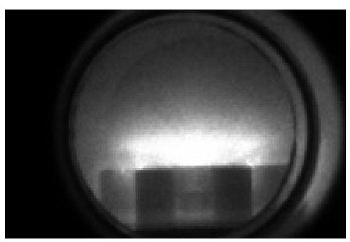

before the pinch

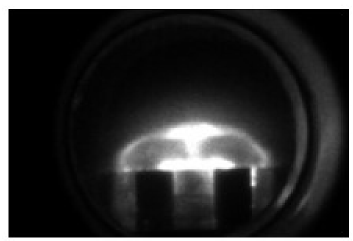

pinch

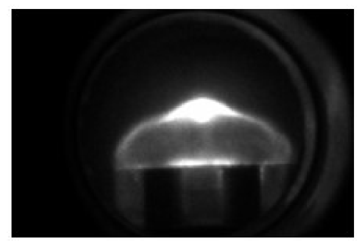

after the pinch

J. Moreno, P. Silva, and L. Soto, Plasma Sources Science and Technology **12**, 39 (2003)

X-rays and neutron detection

Photomultipliers
+
Scintilators

Time of fligth

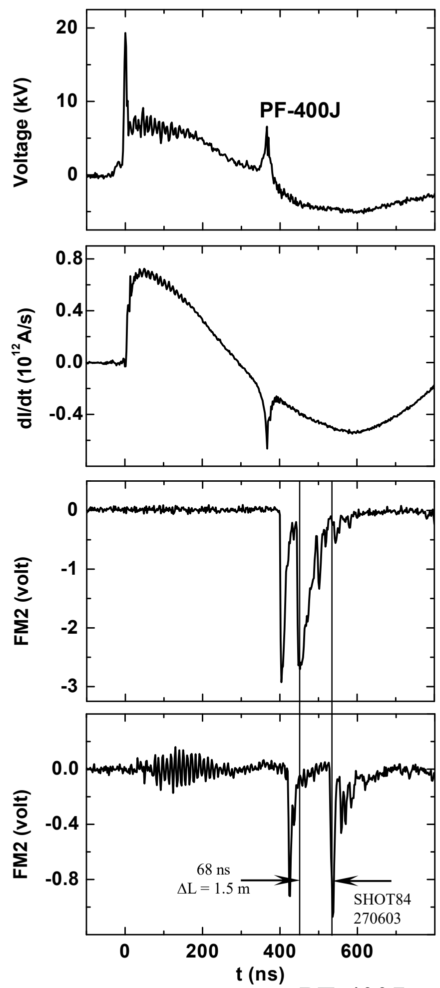

PF-400J

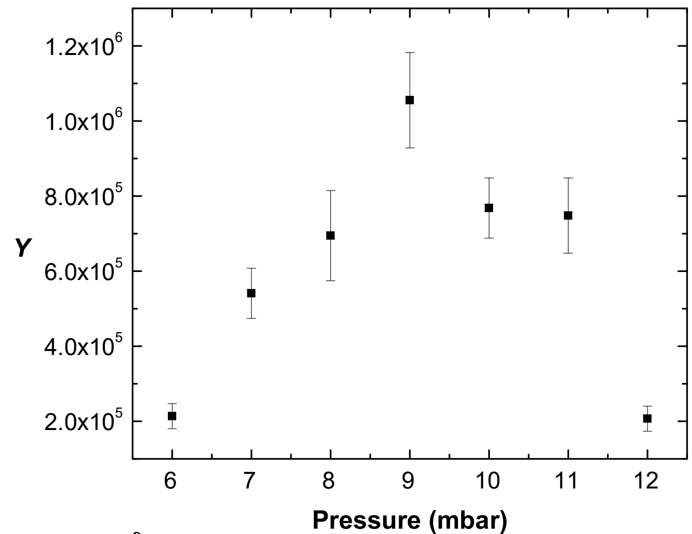

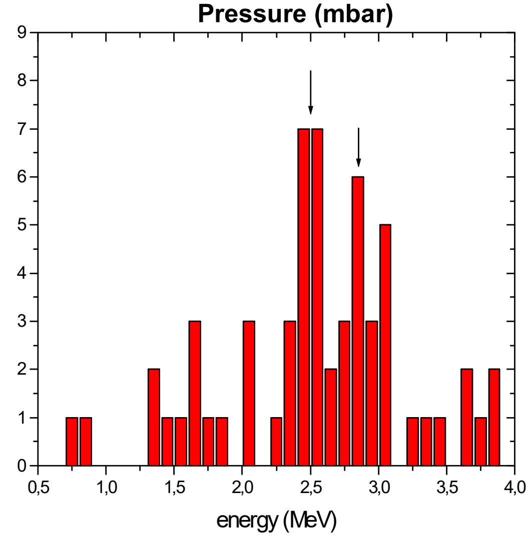

Neutron yield, Y:

Silver activation counters

^{3}He tubes

P. Silva, J. Moreno, L. Soto, L. Birstein, R. Mayer, and W. Kies, App. Phys. Lett. 83, 3269 (2003)

Optical refractive diagnostics

$$\mu_e = 1 - \frac{1}{2}\frac{\omega_p^2}{\omega^2}$$

$$\mu_e - 1 = -4{,}49 \cdot 10^{-16}\,\lambda^2 n_e$$

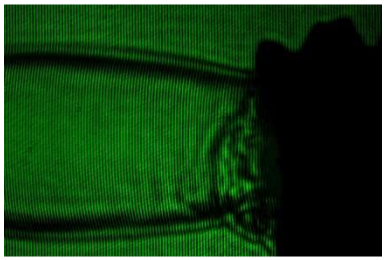

Shadowgraph

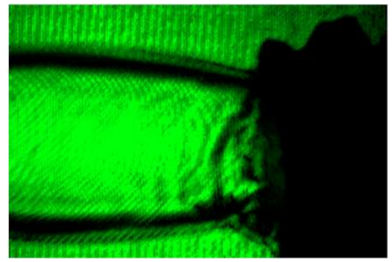

Schlieren

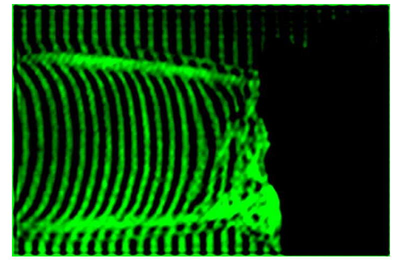

Interferometry

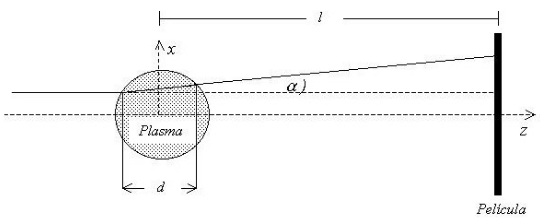

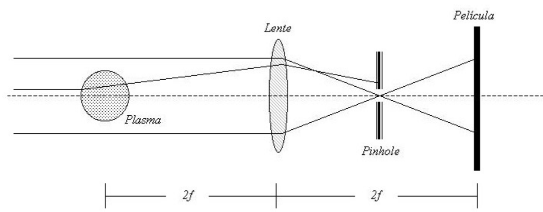

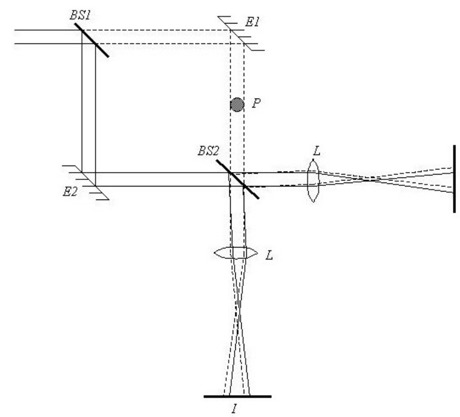

$$\frac{\Delta I}{I} \approx l \int_{z_1}^{z_2} \nabla_\perp^2 \mu(x,y,z)\,dy$$

$$\alpha_x = \int_0^d \frac{1}{\mu}(\partial\mu/\partial x)\,dz$$

$$\Delta\varphi = \frac{2\pi}{\lambda}\int_{x_1}^{x_2} (\mu(x,y,z) - \mu_0)\,dx$$

L. Soto
Plasma Physics and Nuclear Fusion Laboratory
Chilean Nuclear Energy Commission

PF-400J

S#10
-40
S#21
-32
S#08
-18
S#35
-7
S#19
-4
S#36
-2
S#20
12

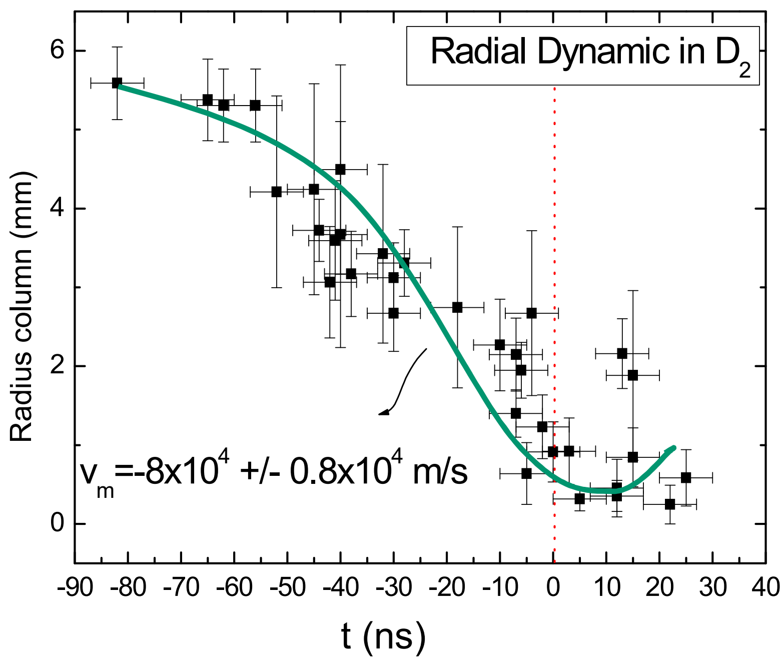

Radial Dynamic in D_2
v_m=-8x10^4 +/- 0.8x10^4 m/s
Radius column (mm)
t (ns)

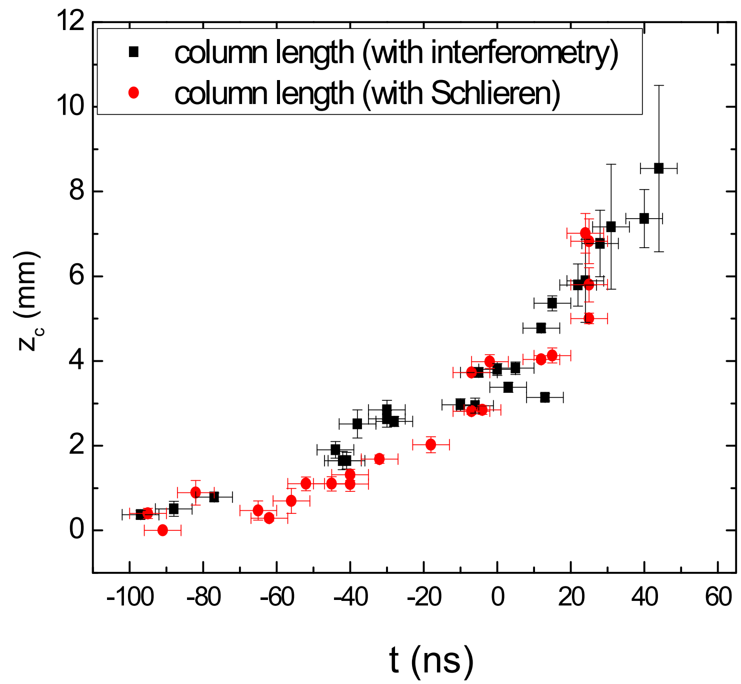

column length (with interferometry)
column length (with Schlieren)
z_c (mm)
t (ns)

PF-400J

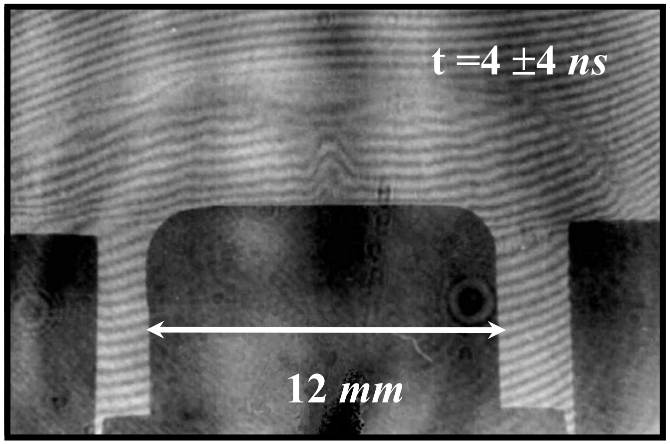

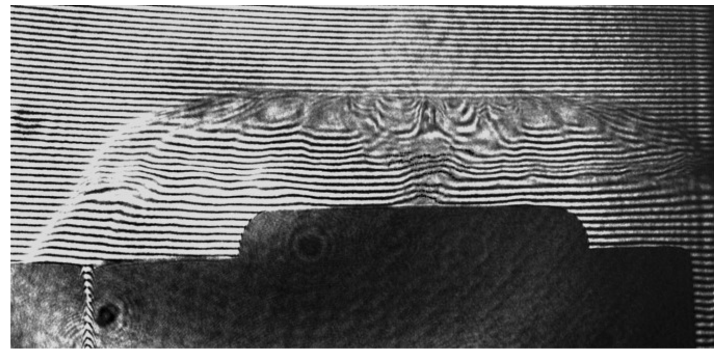

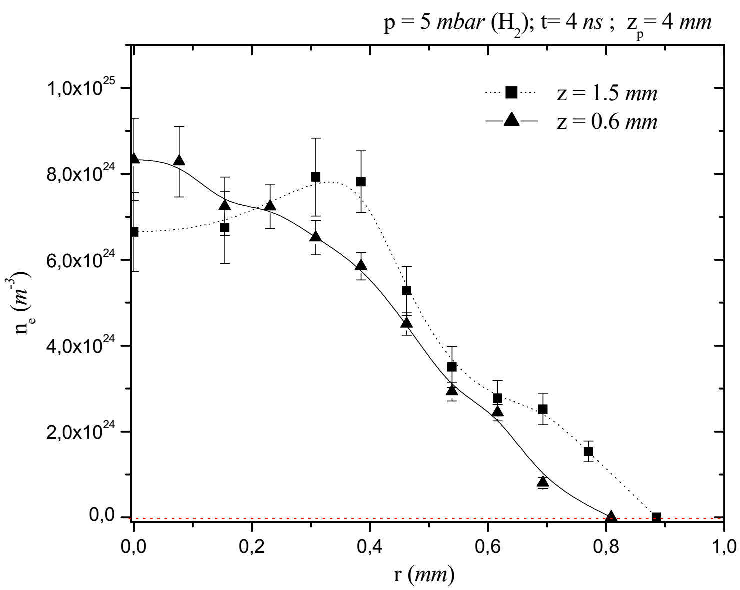

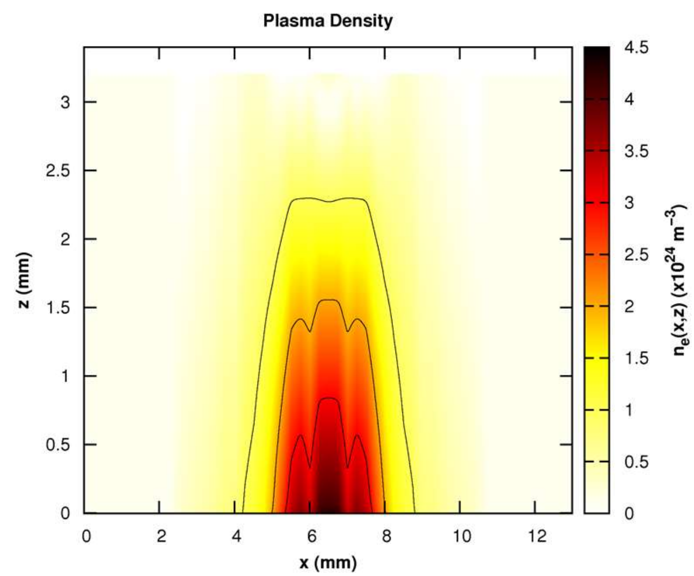

C. Pavez and L. Soto, Physica Scripta **T131**, 014030 (2008)

PF-50J

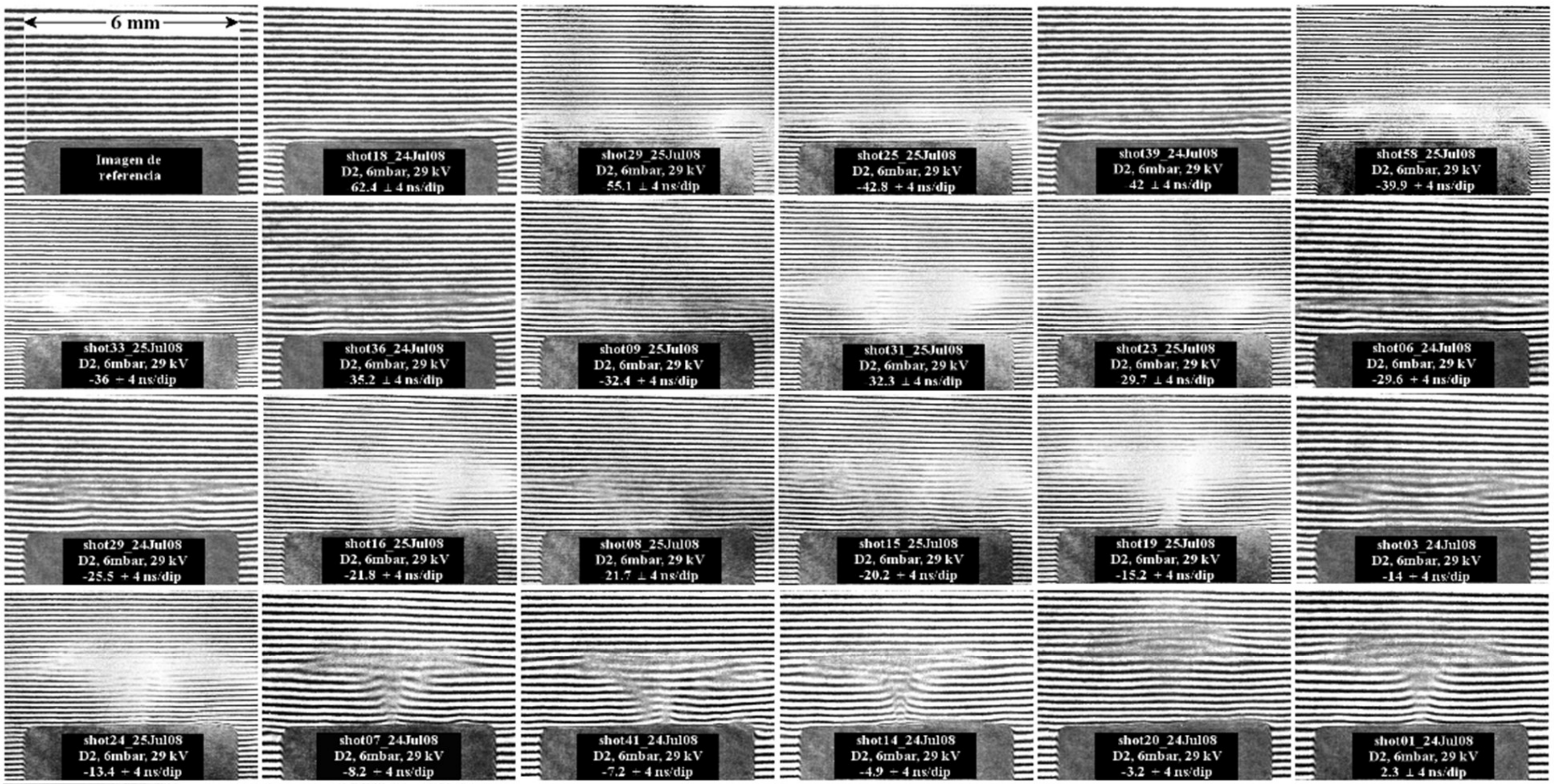

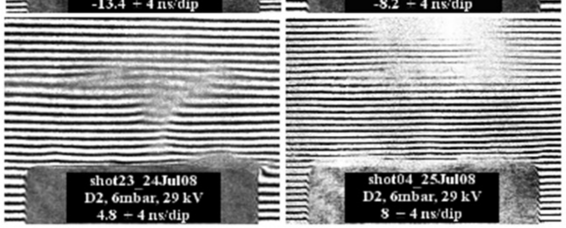

Radial and pinch phase occurs during the last 55ns before the first quarter of period (~150 ns). After column disruption, remaining plasma propagates in the axial direction as a shock wave, but no structure is observed on the axis at the anode end.

A. Tarifeño, C. Pavez, J. Moreno and L. Soto, IEEE Trans. Plasma Science, **39**, 756 (2011)

PF-50J

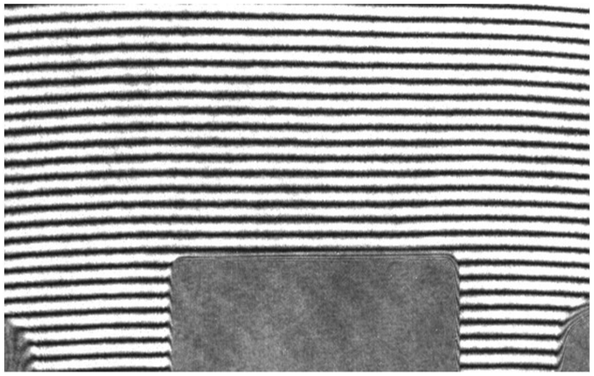

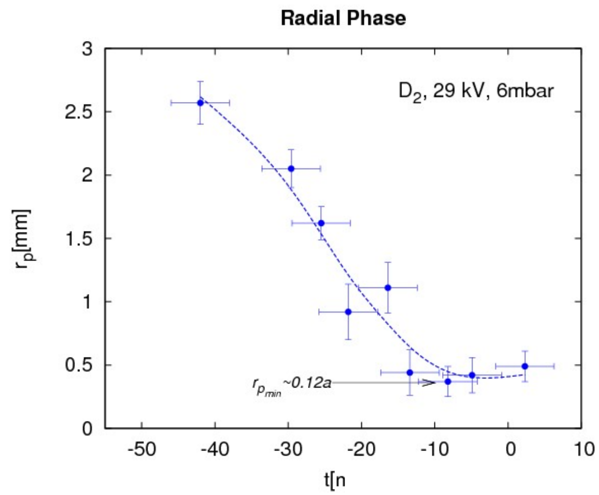

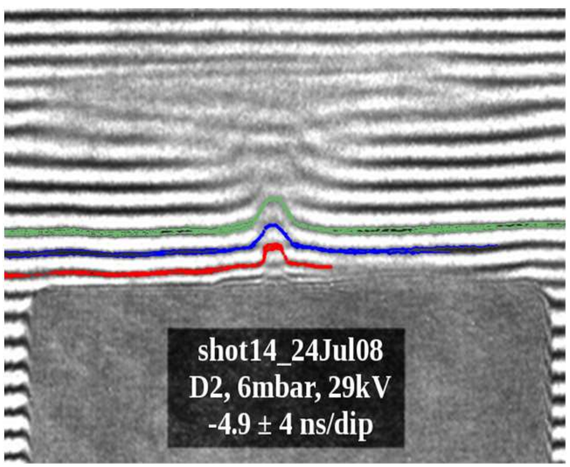

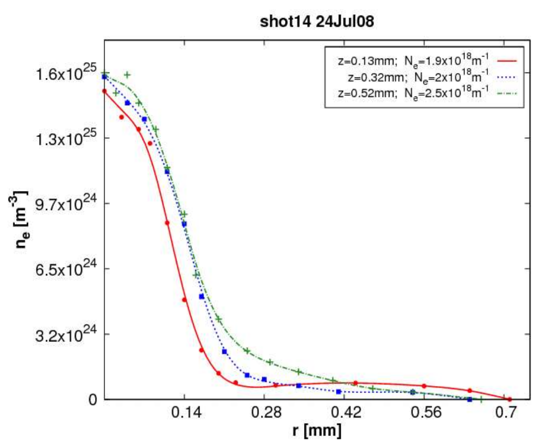

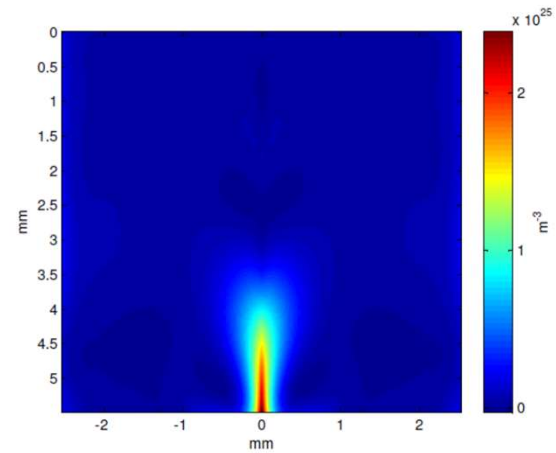

A. Tarifeño, C. Pavez, J. Moreno and L. Soto, IEEE Trans. Plasma Science, **39**, 756 (2011)

J Fusion Energ (2012) 31:279–283
DOI 10.1007/s10894-011-9469-1

ORIGINAL RESEARCH

Toroidal High-Density Singularity in a Small Plasma Focus

Federico Casanova · Ariel Tarifeño-Saldivia ·
Felipe Veloso · Cristian Pavez · Alejandro Clausse ·
Leopoldo Soto

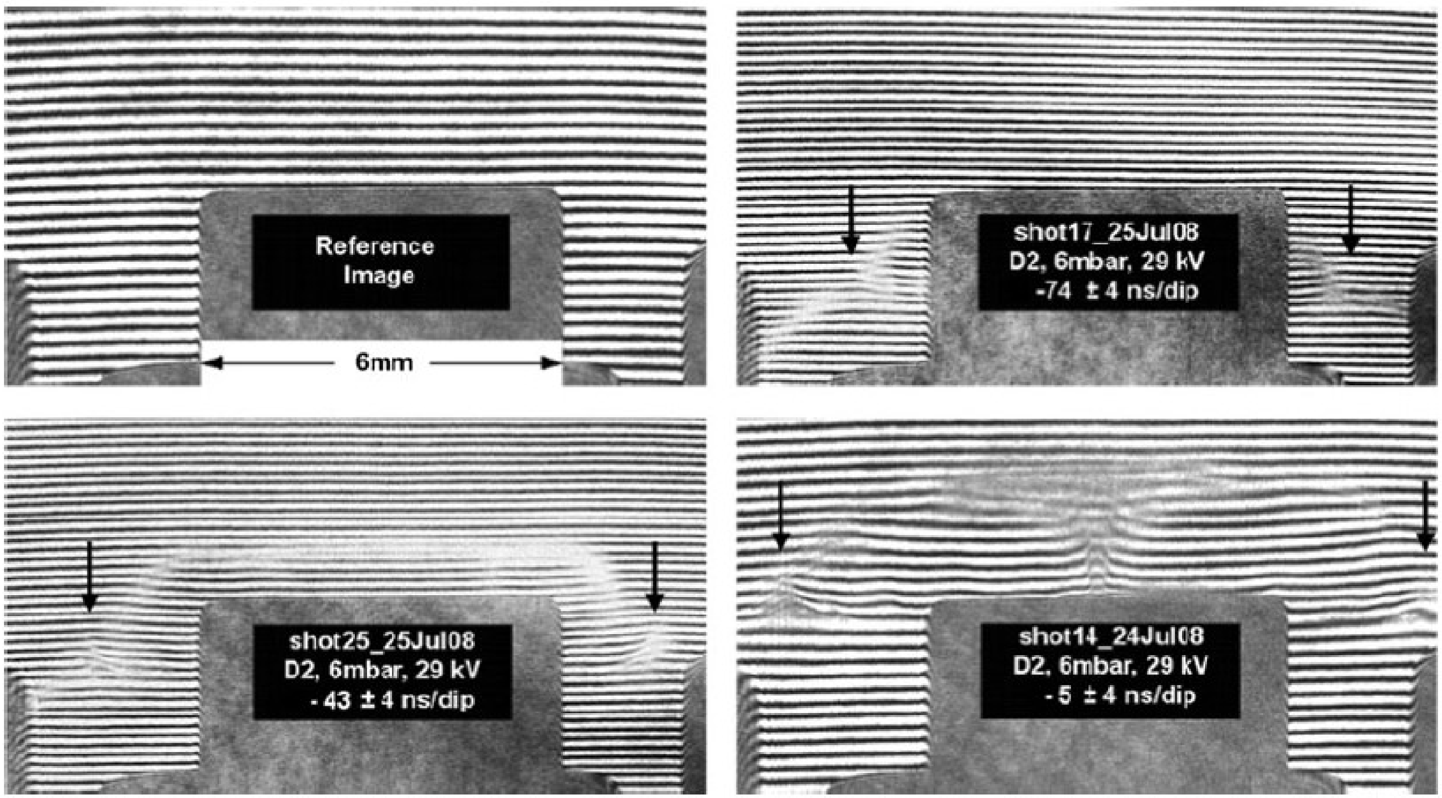

J Fusion Energ (2012) 31:279–283
DOI 10.1007/s10894-011-9469-1

ORIGINAL RESEARCH

Toroidal High-Density Singularity in a Small Plasma Focus

Federico Casanova · Ariel Tarifeño-Saldivia ·
Felipe Veloso · Cristian Pavez · Alejandro Clausse ·
Leopoldo Soto

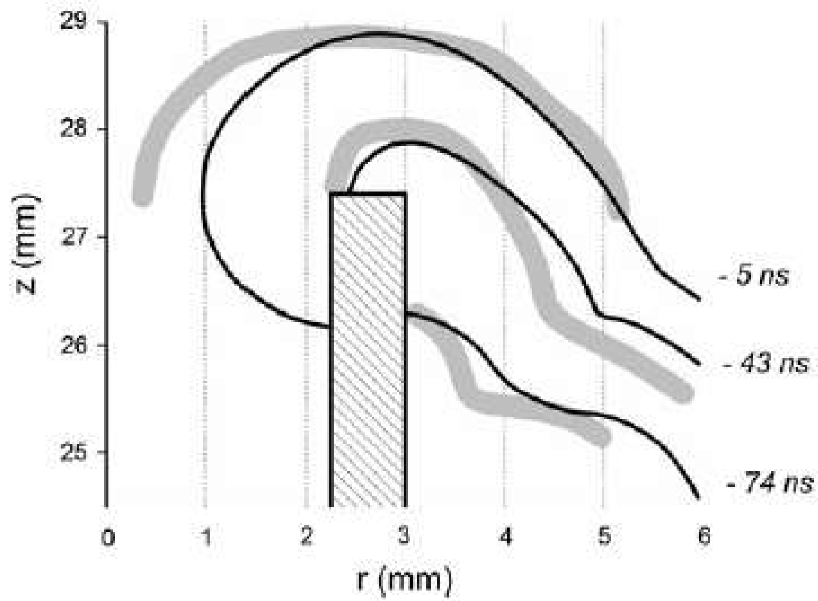

Fig. 5 Shape of the current sheet at different times. Numerical (*black*), experimental (*solid grey*). The *numbers* at the right indicate the corresponding time relative to dip

PHYSICS OF PLASMAS **21**, 072702 (2014)

Filamentary structures in dense plasma focus: Current filaments or vortex filaments?

Leopoldo Soto,[1,2,3,a)] Cristian Pavez,[1,2,3] Fermin Castillo,[4] Felipe Veloso,[5] José Moreno,[1,2,3] and S. K. H. Auluck[6]
[1]*Comisión Chilena de Energía Nuclear, CCHEN, Casilla 188-D, Santiago, Chile*
[2]*Center for Research and Applications in Plasma Physics and Pulsed Power, P⁴*
[3]*Departamento de Ciencias Físicas, Facultad de Ciencias Exactas, Universidad Andrés Bello, República 220, Santiago, Chile*
[4]*Universidad Nacional Autónoma de México, Cuernavaca, México*
[5]*Instituto de Física, Pontificia Universidad Católica de Chile, 7820436 Santiago, Chile*
[6]*Bhabha Atomic Research Center, Mumbai 400 085, India*

PF-400J

Filaments

Visible images

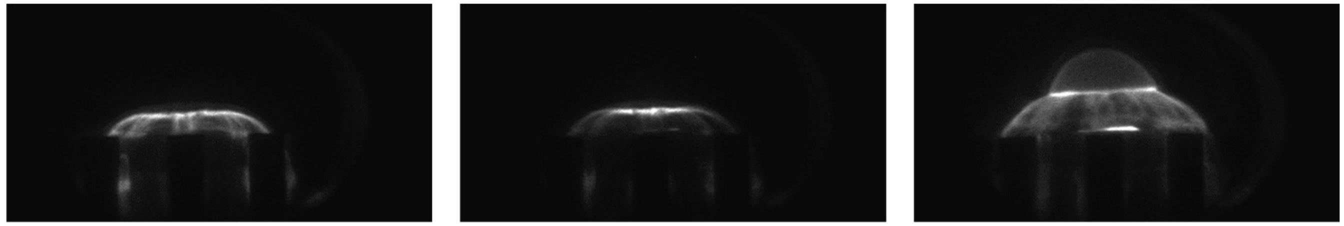

-16ns - 6ns 49ns

Schlieren

Interferogram

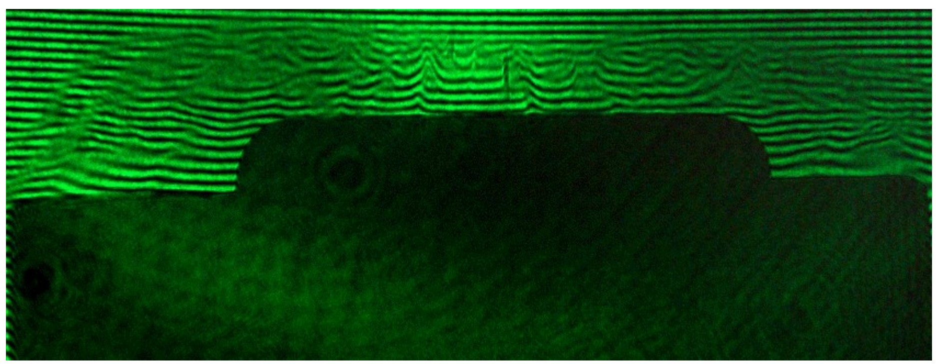

Filaments diameter ~ 300μm, $n_e \sim 10^{25}$ m^{-3}

L. Soto, C. Pavez, F. Castillo, F. Veloso, J. Moreno, S. K. Auluck, Physics of Plasmas 21, 072702 (2014)

IOP Publishing
Plasma Physics and Controlled Fusion
Plasma Phys. Control. Fusion **57** (2015) 035008 (6pp)
doi:10.1088/0741-3335/57/3/035008

Neutron energy distribution and temporal correlations with hard x-ray emission from a hundreds of joules plasma focus device

José Moreno[1,2,3], Felipe Veloso[4], Cristian Pavez[1,2,3], Ariel Tarifeño-Saldivia[1,2,6], Daniel Klir[5] and Leopoldo Soto[1,2,3]

[1] Comisión Chilena de Energía Nuclear, Casilla 188-D, Santiago, Chile
[2] Center for Research and Applications in Plasma Physics and Pulsed Power, P4, Chile
[3] Departamento de Ciencias Físicas, Facultad de Ciencias Exactas, Universidad Andrés Bello, República 220, Santiago, Chile
[4] Instituto de Física, Pontificia Universidad Católica de Chile, Av Vicuña Mackenna 4860, Macul, Santiago, Chile
[5] Department of Physics, Faculty of Electrical Engineering, Czech Technical University, Technicka 2, 16627 Prague 6, Czech Republic

E-mail: jmoreno@cchen.cl

Received 1 October 2014, revised 31 December 2014
Accepted for publication 14 January 2015
Published 18 February 2015

CrossMark

Neutron energy distribution and temporal correlations with hard x-ray emission on 400J

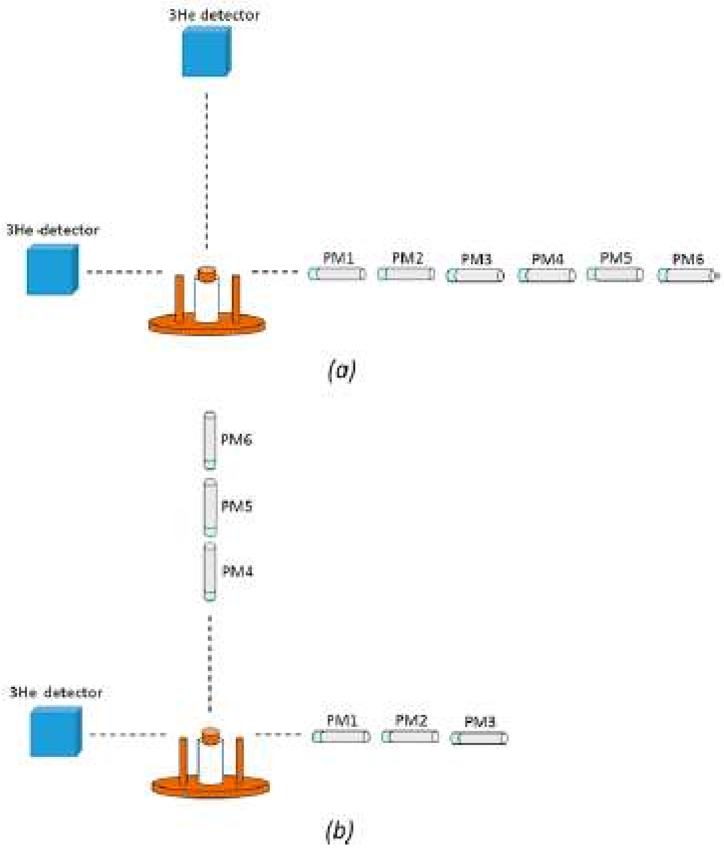

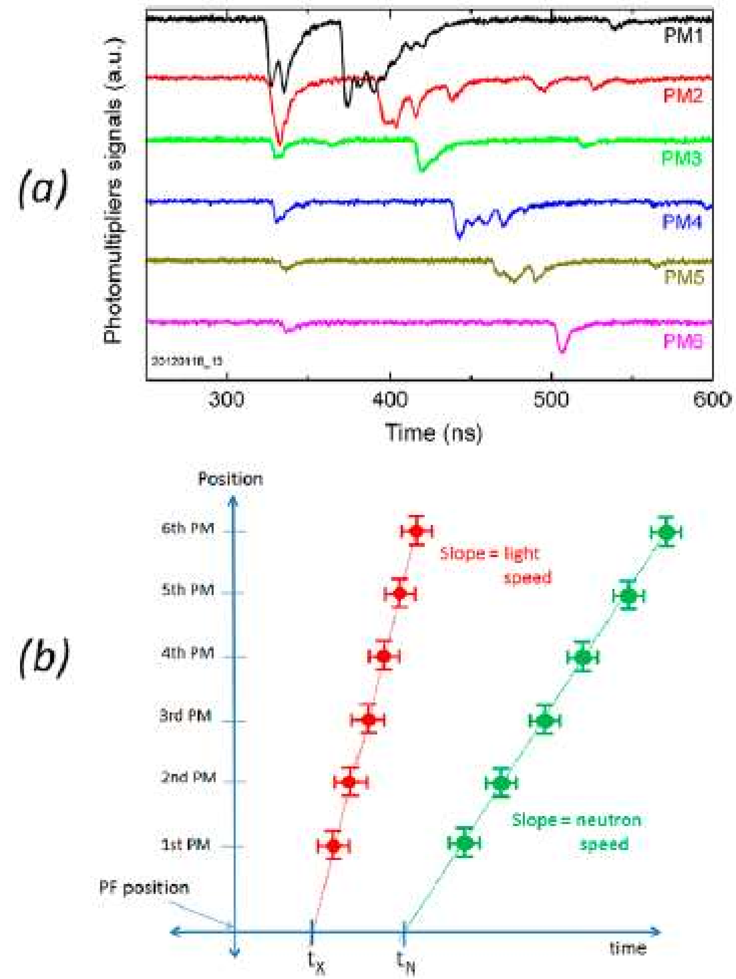

J. Moreno, F. Veloso, C. Pavez, A. Tarifeño-Saldivia, D. Klir, and L. Soto, Plasma Phys. Control. Fusion 57, 035008 (2015)

Neutron energy distribution and temporal correlations with hard x-ray emission on PF-400J

A

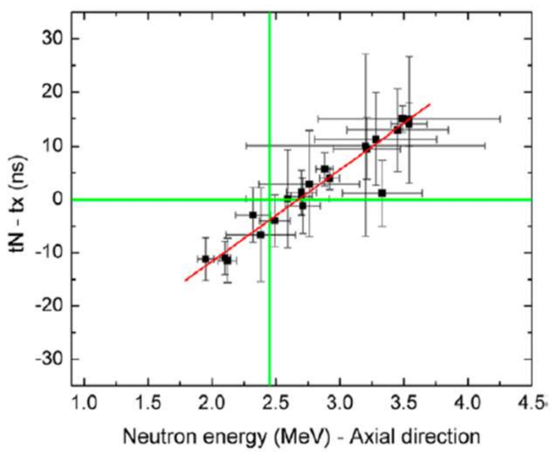

C

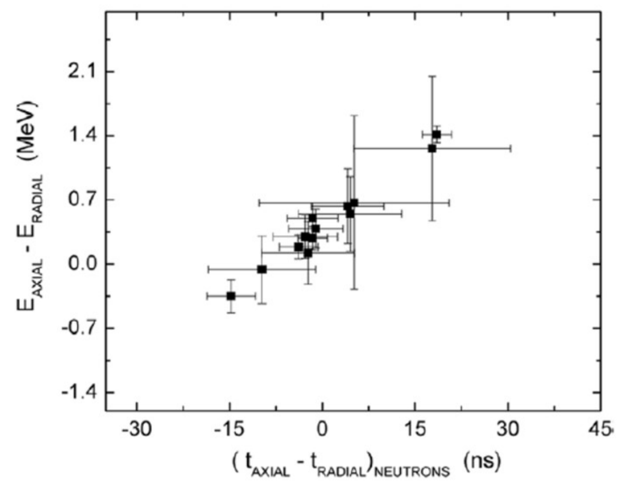

B

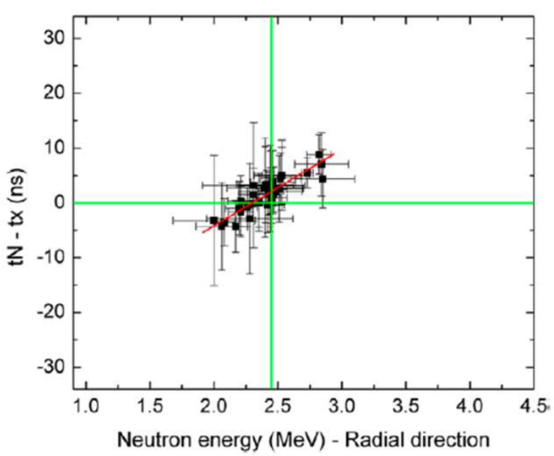

These results not only show differences in the production time of hard x-rays and neutrons, but also some correlation on the neutron energy and the $t_N - t_X$ time difference in both directions (i.e., the larger neutron energy corresponds to later times with respect to hard x-rays emission).

The axial-to-radial ratio of both total neutron yield and neutron energies indicates anisotropic emission, which is consistent with a 100 keV kinetic energy of the deuterons in the axial direction. The energy spread among different shots was ~0.5 MeV in the axial direction which is 2.5 times the spread in the radial direction. Furthermore, temporal differences on hard x-rays and neutron production over each direction are found. These differences show correlation with neutron energies. This could be related to the existence of two temporally separated neutron production times corresponding to different moments during the plasma focus discharge.

J. Moreno, F. Veloso, C. Pavez, A. Tarifeño-Saldivia, D. Klir, and L. Soto, Plasma Phys. Control. Fusion 57, 035008 (2015)

PHYSICS OF PLASMAS **21**, 122703 (2014)

Characterization of the axial plasma shock in a table top plasma focus after the pinch and its possible application to testing materials for fusion reactors

Leopoldo Soto,[1,2,3,a)] Cristian Pavez,[1,2,3] José Moreno,[1,2,3] María José Inestrosa-Izurieta,[1,2] Felipe Veloso,[4] Gonzalo Gutiérrez,[5] Julio Vergara,[6] Alejandro Clausse,[7] Horacio Bruzzone,[8] Fermín Castillo,[9] and Luis F. Delgado-Aparicio[10]

[1]*Comisión Chilena de Energía Nuclear, Casilla 188-D, Santiago, Chile*
[2]*Centro de Investigación y Aplicaciones en Física de Plasmas y Potencia Pulsada, P[4], Santiago-Talca, Chile*
[3]*Departamento de Ciencias Físicas, Facultad de Ciencias Exactas, Universidad Andrés Bello, República 220, Santiago, Chile*
[4]*Instituto de Física, Pontificia Universidad Católica de Chile, Santiago, Chile*
[5]*Departamento de Física, Facultad de Ciencias, Universidad de Chile, Santiago, Chile*
[6]*Facultad de Ingeniería, Pontificia Universidad Católica de Chile, Santiago, Chile*
[7]*CNEA-CONICET and Universidad Nacional del Centro, 7000 Tandil, Argentina*
[8]*CONICET and Universidad de Mar del Plata, Mar del Plata, Argentina*
[9]*Instituto de Ciencias Físicas, Universidad Nacional Autónoma de México, Cuernavaca, Morelos, Mexico*
[10]*Princeton Plasma Physics Laboratory, Princeton University, Princeton, New Jersey 08543, USA*

(Received 19 September 2014; accepted 20 November 2014; published online 5 December 2014)

Plasma bursts after the pinch

Previus studies did not pay atention after the pinch disruptions

PF- 400J D_2 9mbar

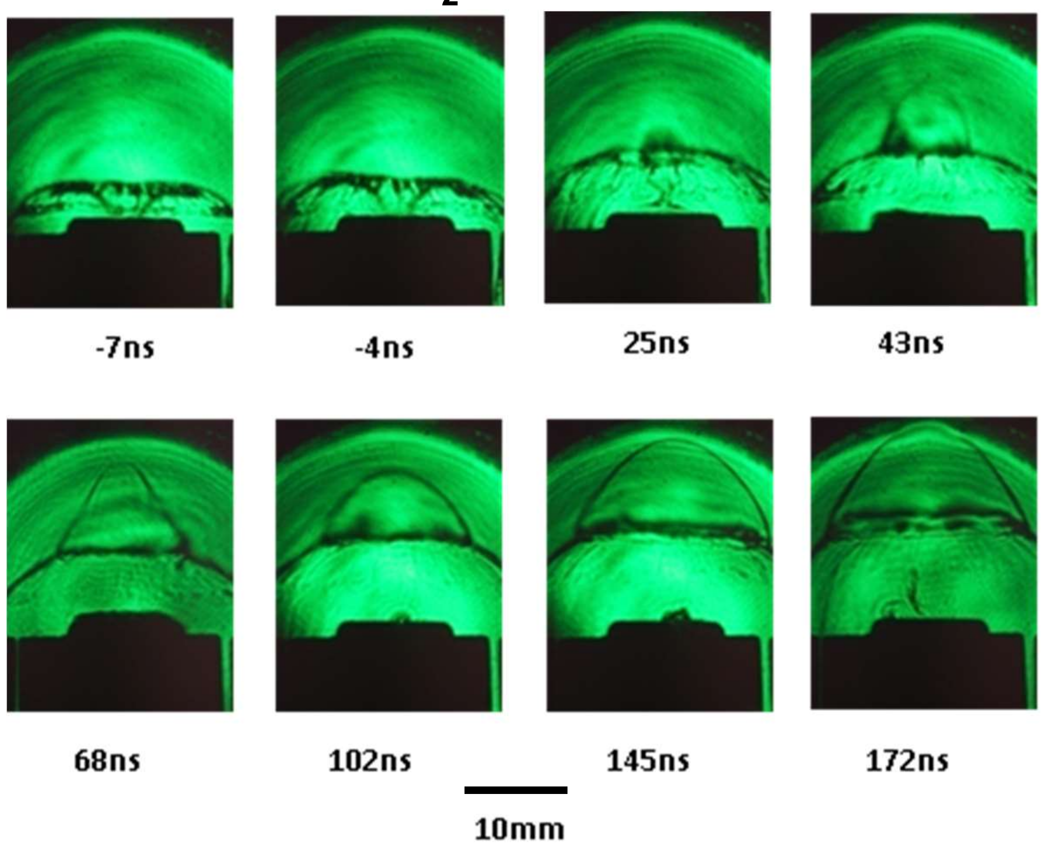

L. Soto, C. Pavez, J. Moreno, M. J. Inestrosa, F. Veloso, G. Gutierrez, J. Vergara, F. Castillo, A. Clausse, H. Bruzzone and L. Delgado-Aparicio, Physics of Plasmas 21, 122703 (2014)

Plasma bursts after the pinch

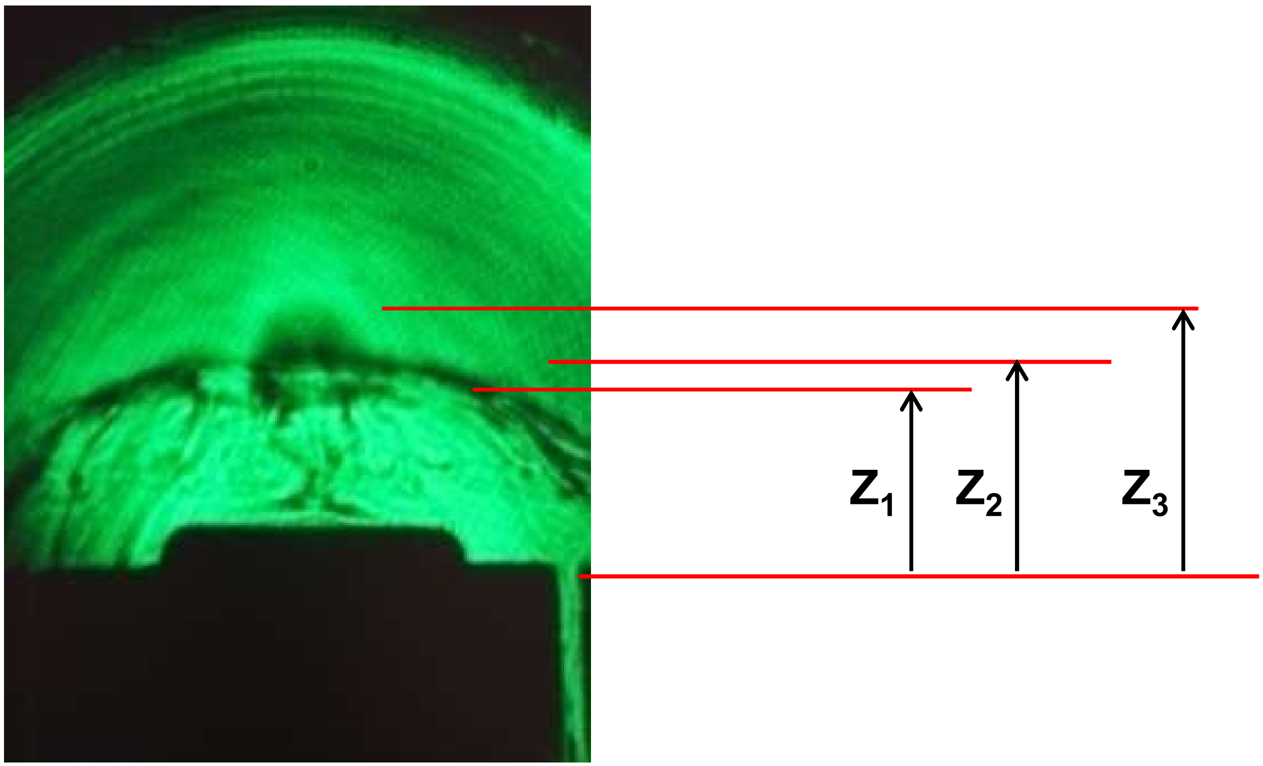

L. Soto, C. Pavez, J. Moreno, M. J. Inestrosa, F. Veloso, G. Gutierrez, J. Vergara, F. Castillo, A. Clausse, H. Bruzzone and L. Delgado-Aparicio, Physics of Plasmas 21, 122703 (2014)

Plasma bursts after the pinch

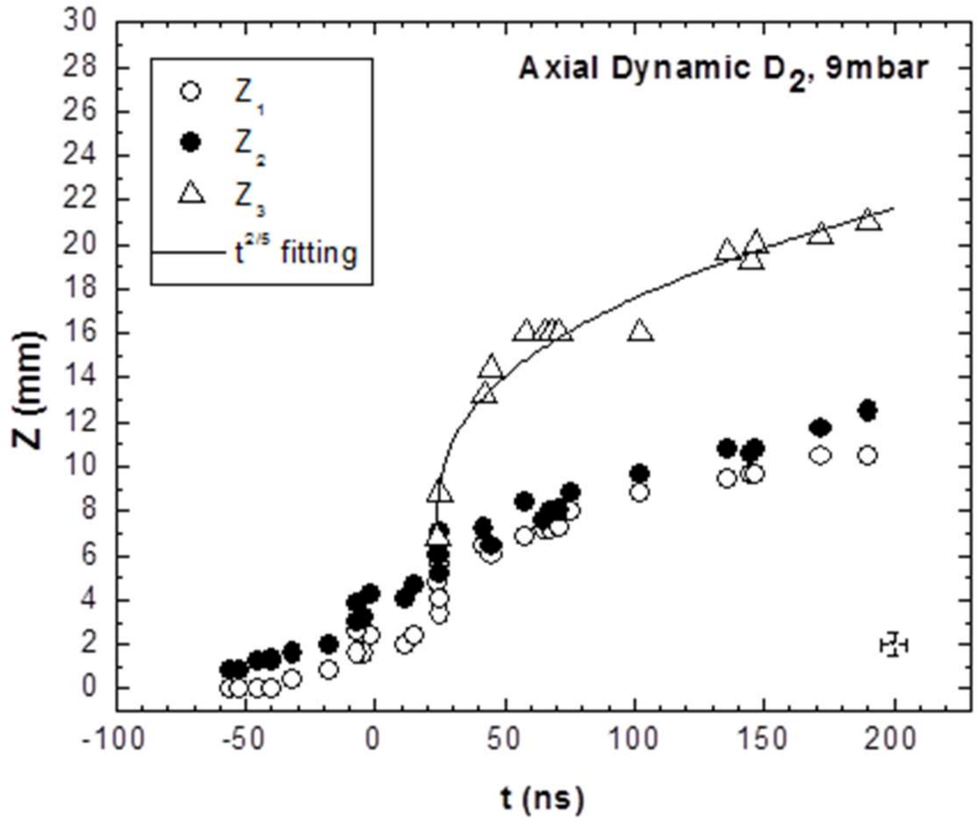

$$Z_3(t) - Z_3(t_0) = \left[\frac{75}{16\pi}\frac{(\gamma-1)(1+\gamma)^2}{(3\gamma-1)}\frac{E}{\rho_0}\right]^{\frac{1}{5}}(t-t_0)^{2/5}$$

L. Soto, C. Pavez, J. Moreno, M. J. Inestrosa, F. Veloso, G. Gutierrez, J. Vergara, F. Castillo, A. Clausse, H. Bruzzone and L. Delgado-Aparicio, Physics of Plasmas 21, 122703 (2014)

PHYSICS OF PLASMAS **22**, 040705 (2015)

Observation of plasma jets in a table top plasma focus discharge

Cristian Pavez,[1,2,3] José Pedreros,[1,4] Ariel Tarifeño-Saldivia,[1,2,a)] and Leopoldo Soto[1,2,3,b)]
[1]*Comisión Chilena de Energía Nuclear, CCHEN, Casilla 188-D, Santiago, Chile*
[2]*Center for Research and Applications in Plasma Physics and Pulsed Power, P4, Santiago-Talca, Chile*
[3]*Departamento de Ciencias Físicas, Facultad de Ciencias Exactas, Universidad Andrés Bello, República 220, Santiago, Chile*
[4]*Departamento de Ingeniería Eléctrica, Universidad de Santiago de Chile, Santiago, Chile*

(Received 2 October 2014; accepted 15 April 2015; published online 24 April 2015)

After plasma jets are observed

PF-50J

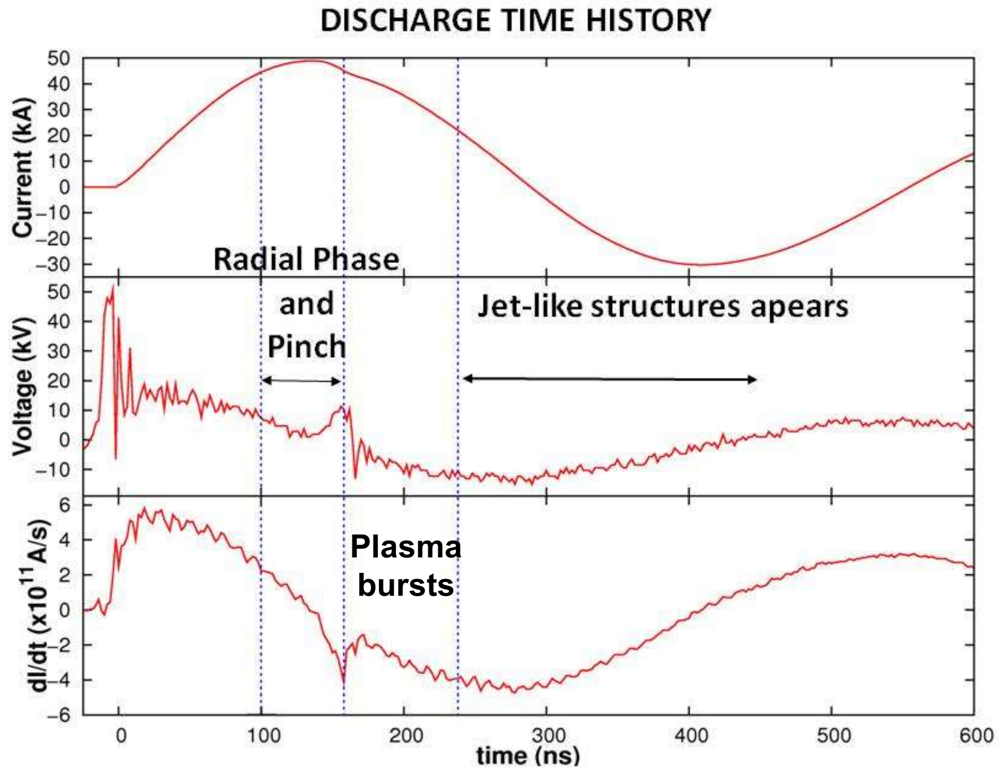

After plasma jets are observed

Hollow anode

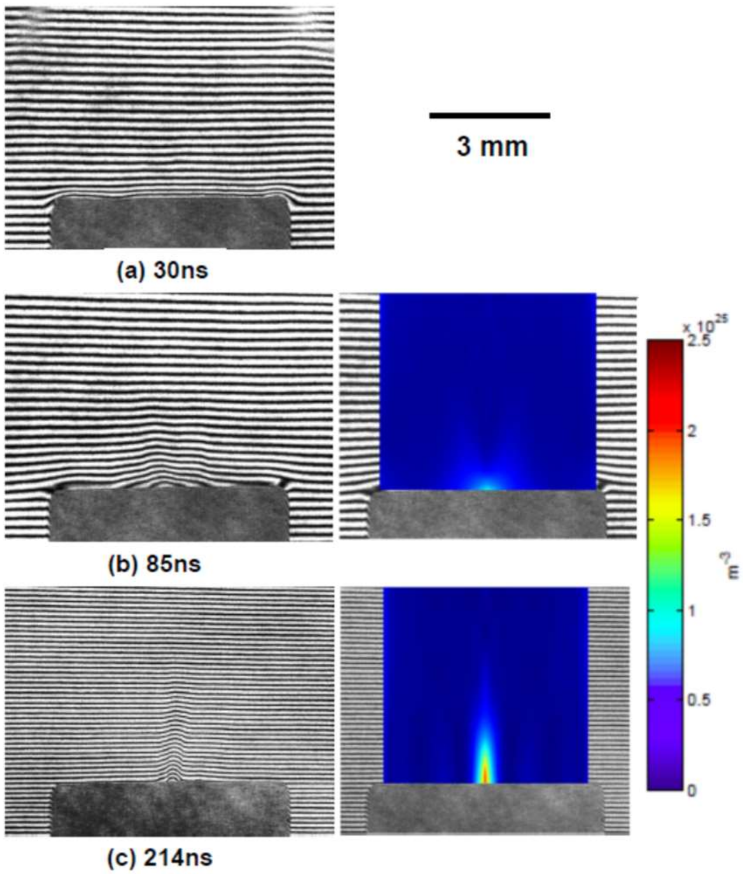

Details of diagnostic in C. Pavez et al, FPPT-8

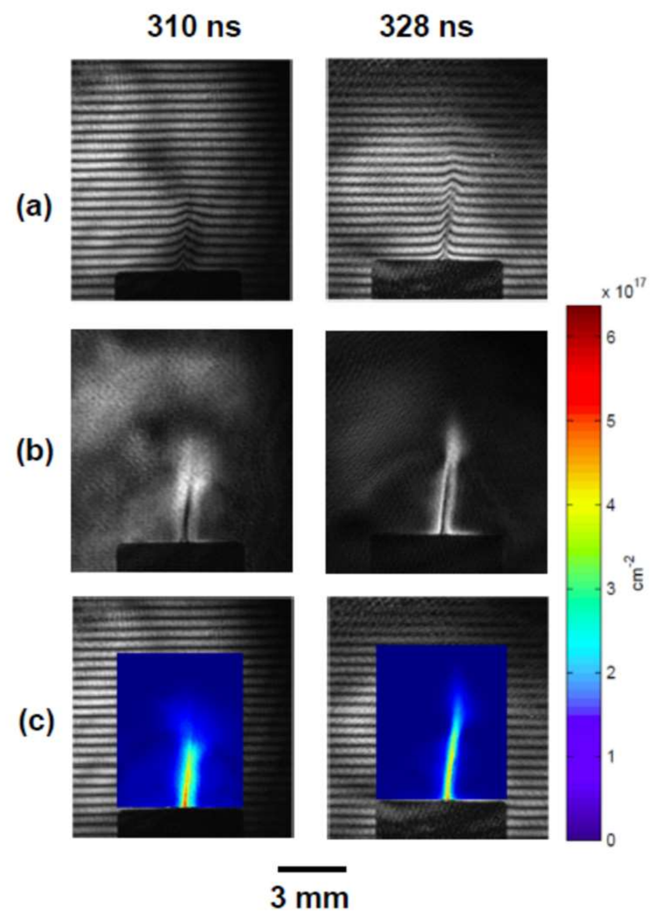

$n_e \sim 10^{24}$ - 10^{25} m^{-3} v~ 4 x 10^4 m/s

C. Pavez, J. Pedreros, A Tarifeño-Saldivia and L. Soto, Physics of Plasmas 22, 040705 (2015)

Plasma jets

Solid anode

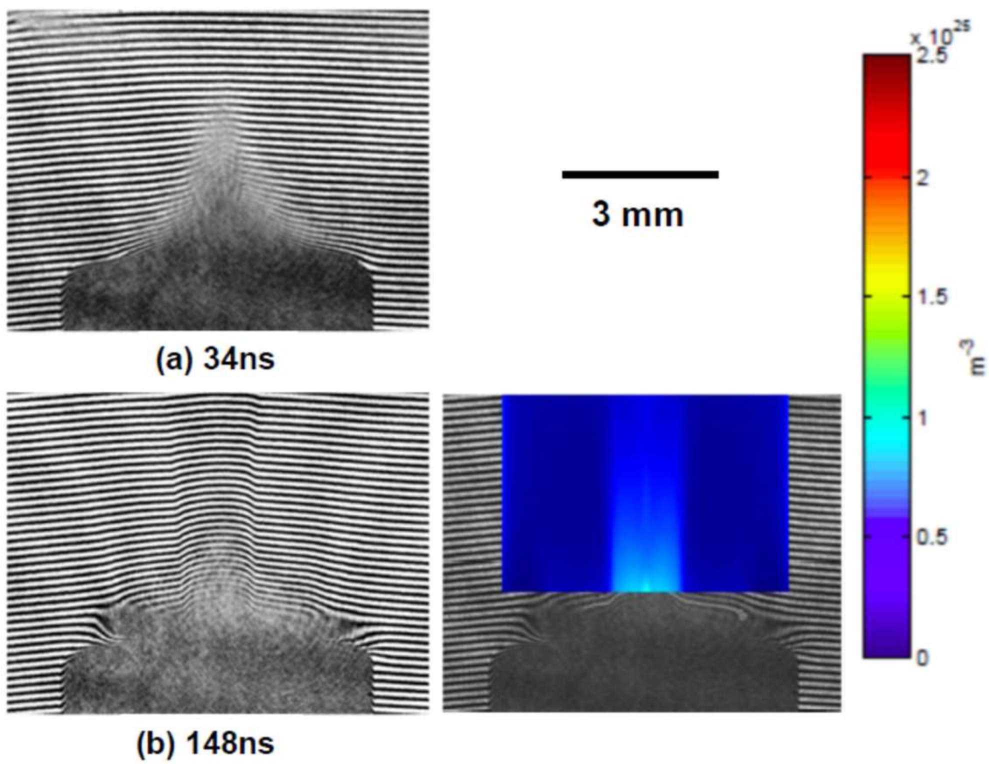

$n_e \sim 10^{24} - 10^{25}\ m^{-3}$ $v \sim 4 \times 10^4$ m/s

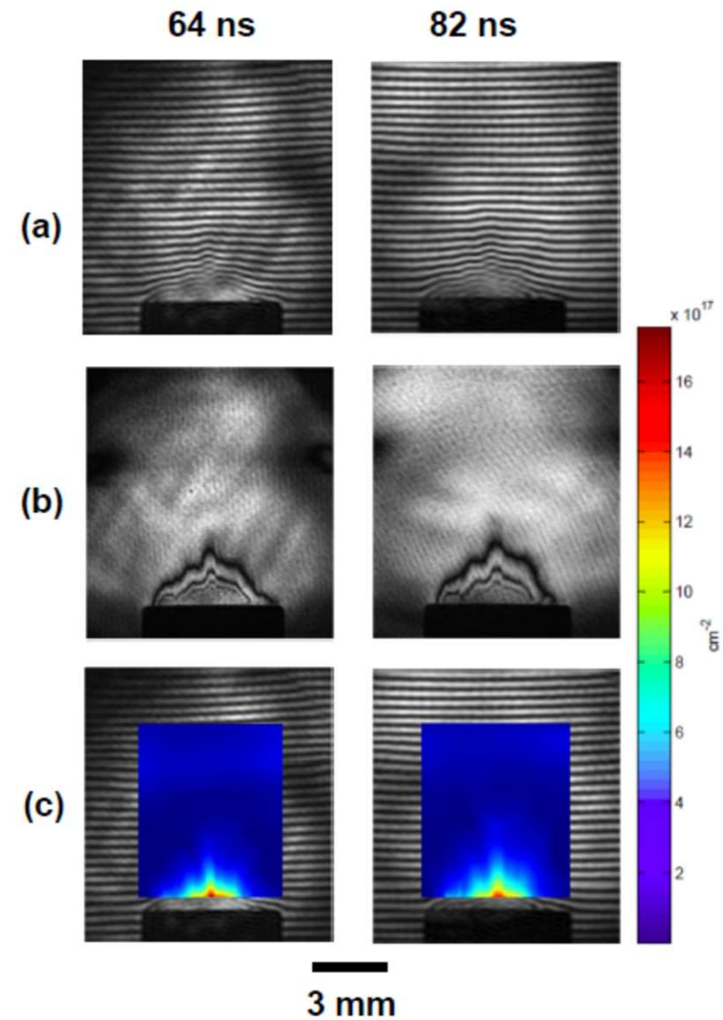

C. Pavez, J. Pedreros, A Tarifeño-Saldivia and L. Soto, Physics of Plasmas 22, 040705 (2015)

PF dynamics including times after the pinch disruption

Plasma Focus Aplications

L. Soto
Plasma Physics and Nuclear Fusion Laboratory
Chilean Nuclear Energy Commission

- X-ray pulses, ns
- Neutron pulses, ns
- Filaments
- Plasma shocks
- Jets

L. Soto
Plasma Physics and Nuclear Fusion Laboratory
Chilean Nuclear Energy Commission

Hard X-ray nanoflash

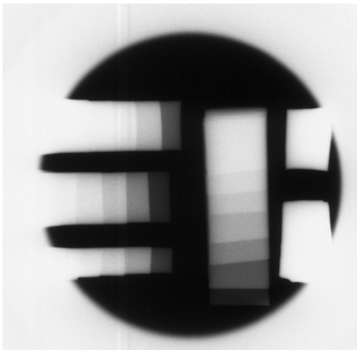

X-ray from PF-400J

~ 90±5 keV energy

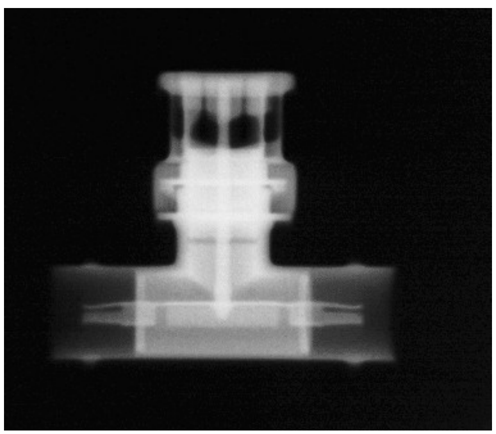

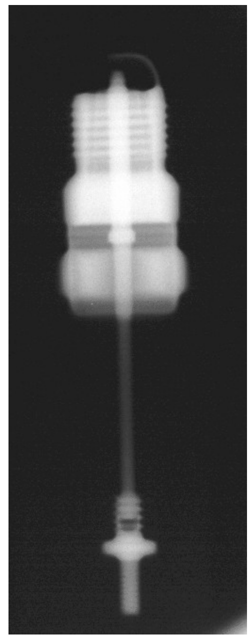

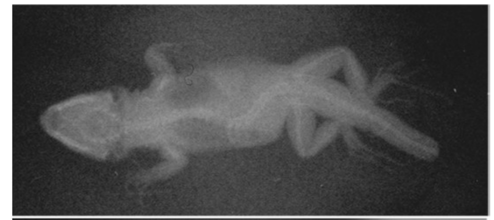

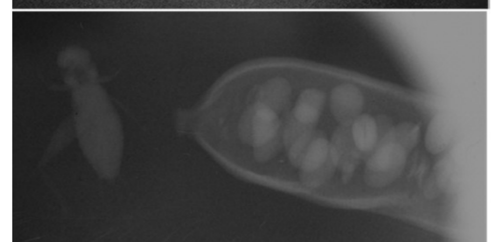

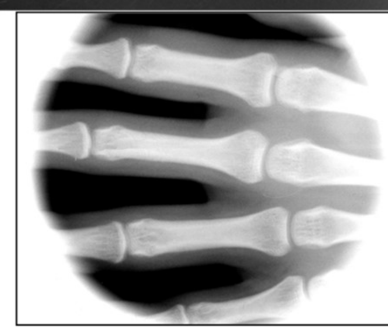

M. Zambra, P. Silva, M. Moreno, C. Pavez and L. Soto, Plasma Physics Controlled Fusion 51, 125003 (2009)
C Pavez, J. Pedreros, M Zambra, F Veloso, J Moreno, A Tarifeño-Saldivia and L. Soto, Plasma Phys. and Control. Fusion. 54 105018 (2012)

A PF for field applications

Motivation

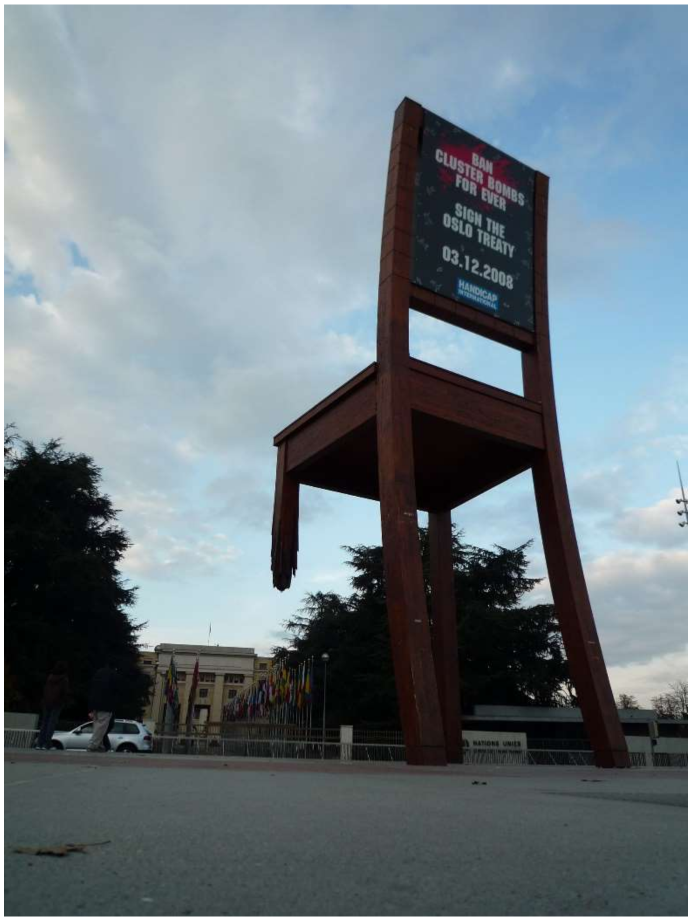

Development of a confirmation method using the neutron backscattering technique for detection of landmines in arid soils

TC IAEA Project

A portable PF device as neutron source for field applications, PF-2J

HYDAD-D at a simulated field with hydrogenated objects under controlled conditions

Arica, Atacama desert, North of Chile, September 11, 2009

C. Pavez, F. D. Brooks, F. D Smit, J. Moreno, L. Altamirano, L. Soto "Tests of the HYDAD Landmine Detector on Dry Soil in Northen Chile, VII Latin American Symposium on Nuclear Physics and Applications, Santiago, Chile, Dec. 2009.

Appications to study materials for fusion reactors

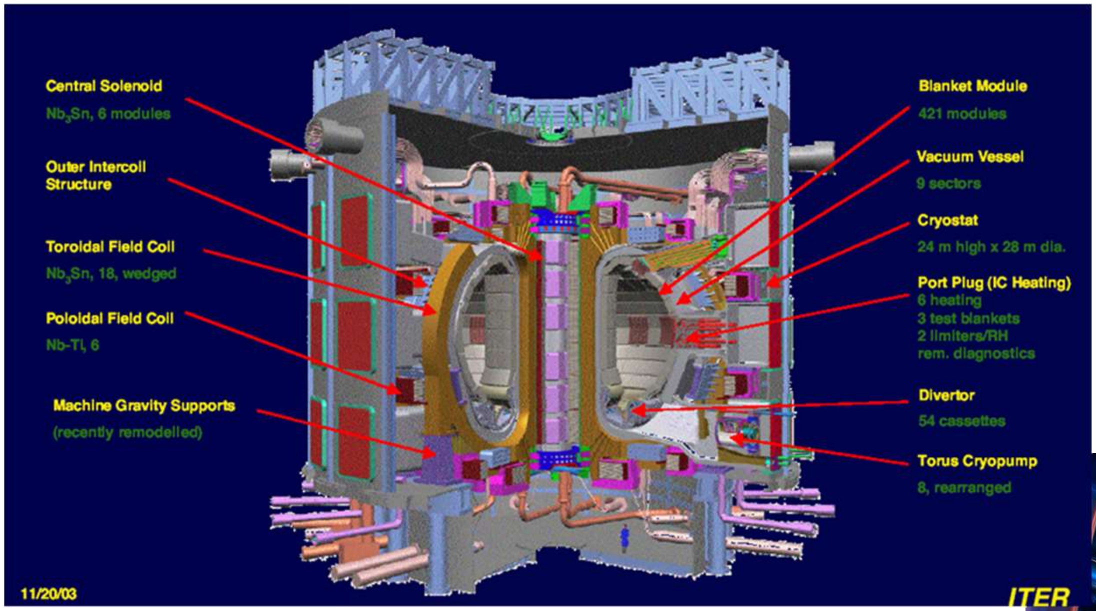

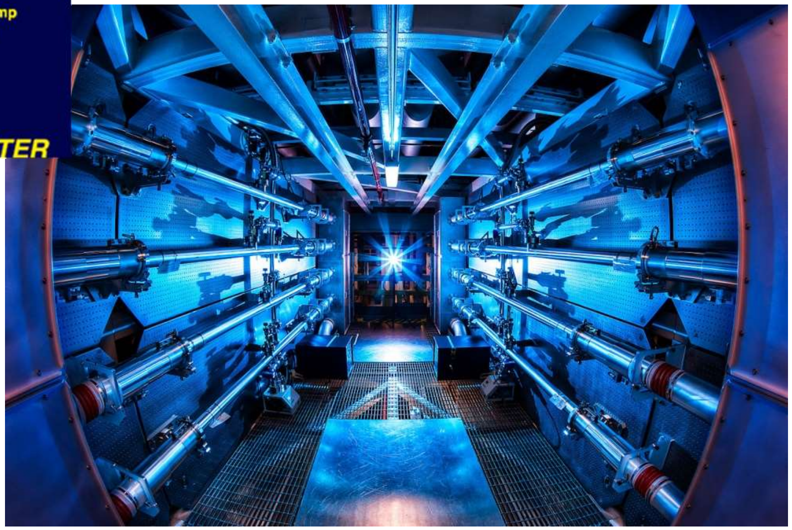

L. Soto
Plasma Physics and Nuclear Fusion Laboratory
Chilean Nuclear Energy Commission

Damage factor

$$F \sim q \cdot \tau^{1/2} = E/S\tau^{1/2}$$

q: power flux, τ: interaction time, S: interaction area

L. Soto
Plasma Physics and Nuclear Fusion Laboratory
Chilean Nuclear Energy Commission

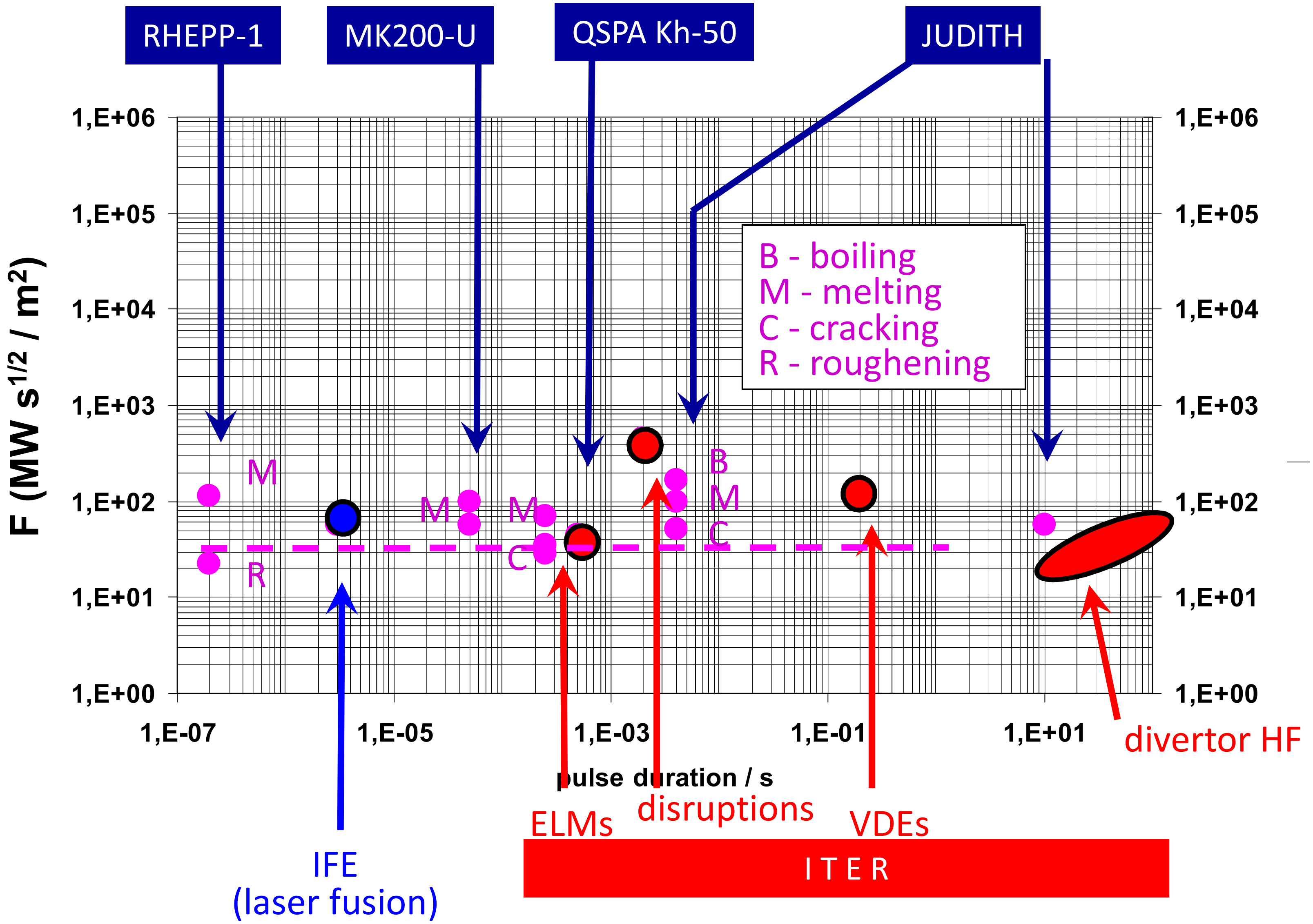

J. Linke et al, J. Nuclear Mat. 367-370, 1422 (2007)

Expected Damage in Fusion Reactor

ITER:

$$F \sim q \cdot \tau^{1/2} \sim 10^8 (W/m^2)\, s^{1/2} = 10^4 (W/cm^2)\, s^{1/2}$$

at 0.5 – 1 Hz , 10^3 pulses

IFE:

$$F \sim q \cdot \tau^{1/2} \sim 10^4 (W/cm^2)\, s^{1/2}$$

at 10 Hz

PF-400J:

$$F \sim q \cdot \tau^{1/2} \sim 10^3 - 10^5 (W/cm^2)\, s^{1/2}$$

at 0.05 Hz

L. Soto
Plasma Physics and Nuclear Fusion Laboratory
Chilean Nuclear Energy Commission

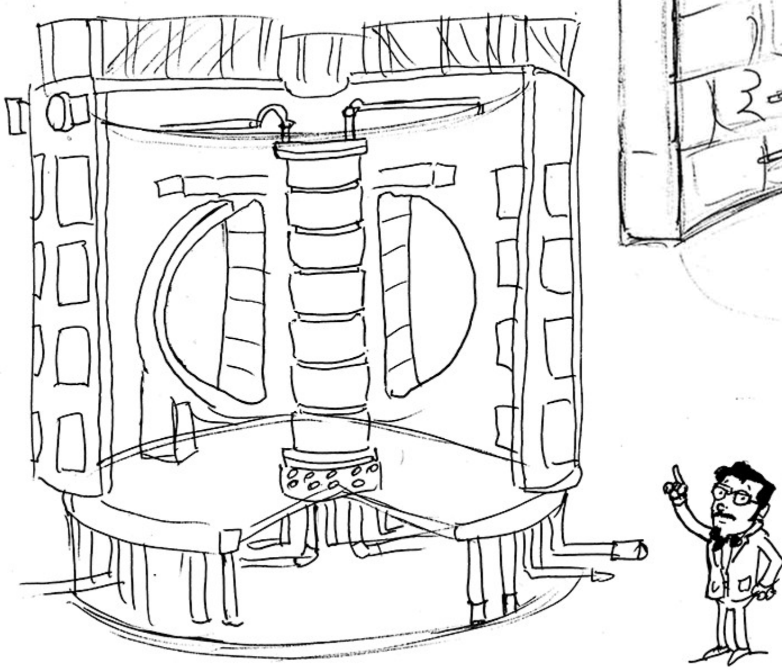

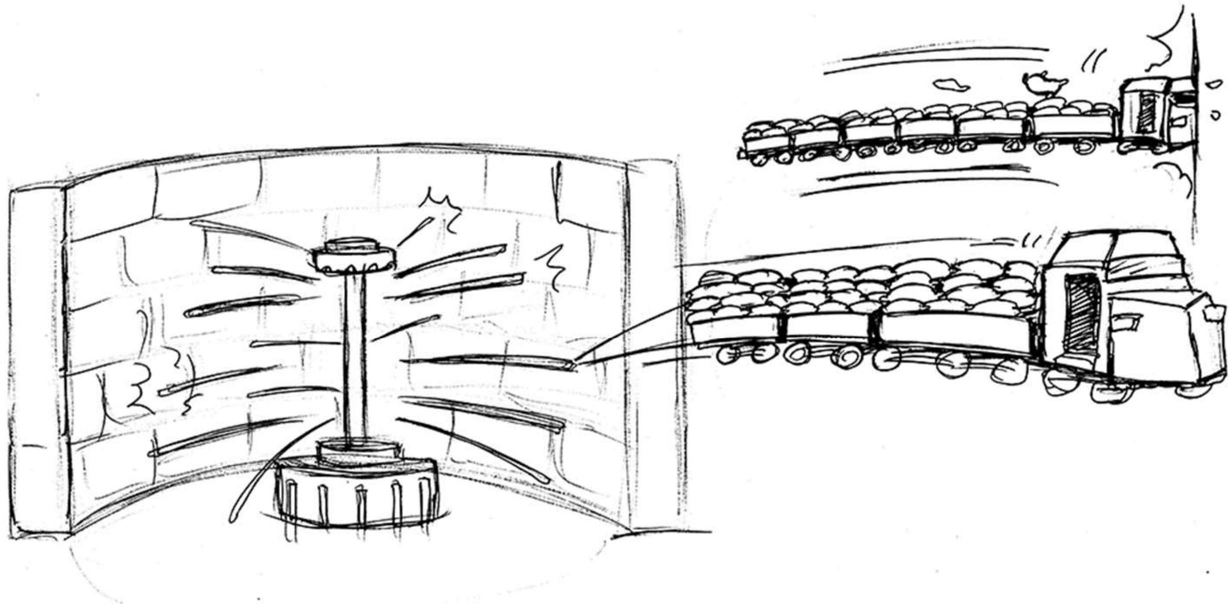

1 ELMs would be "equivalent" to a vagon of train of 100 tons at 220 km/h shocking on a wall

L. Soto
Plasma Physics and Nuclear Fusion Laboratory
Chilean Nuclear Energy Commission

Advanced Materials

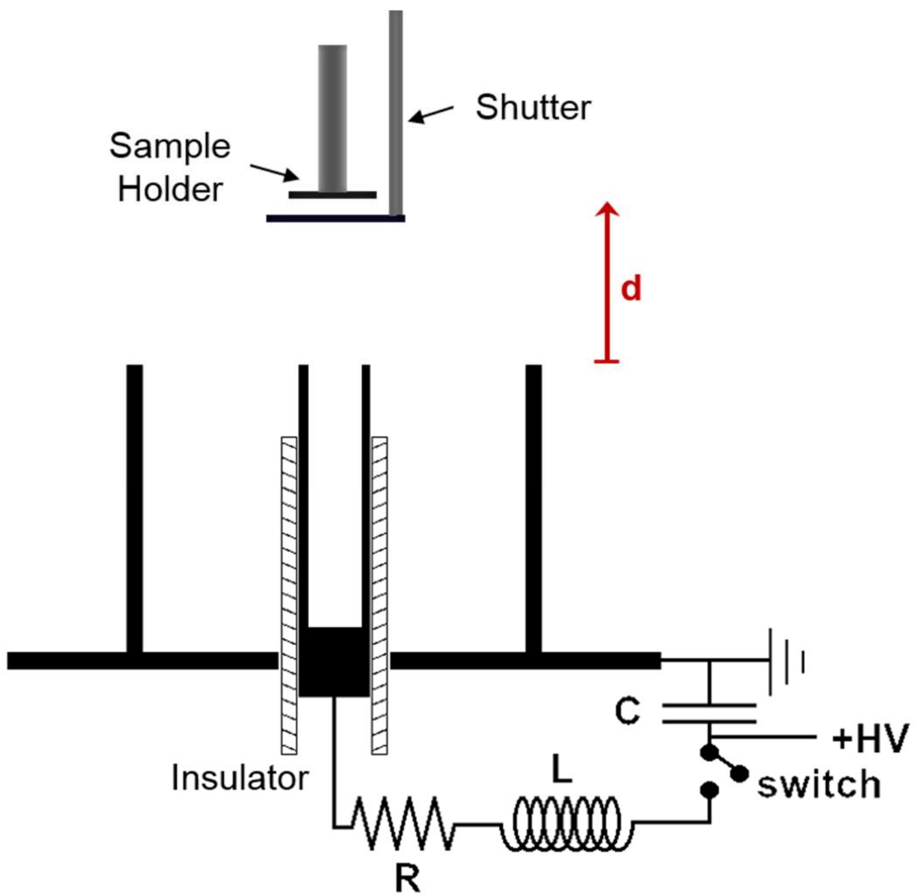

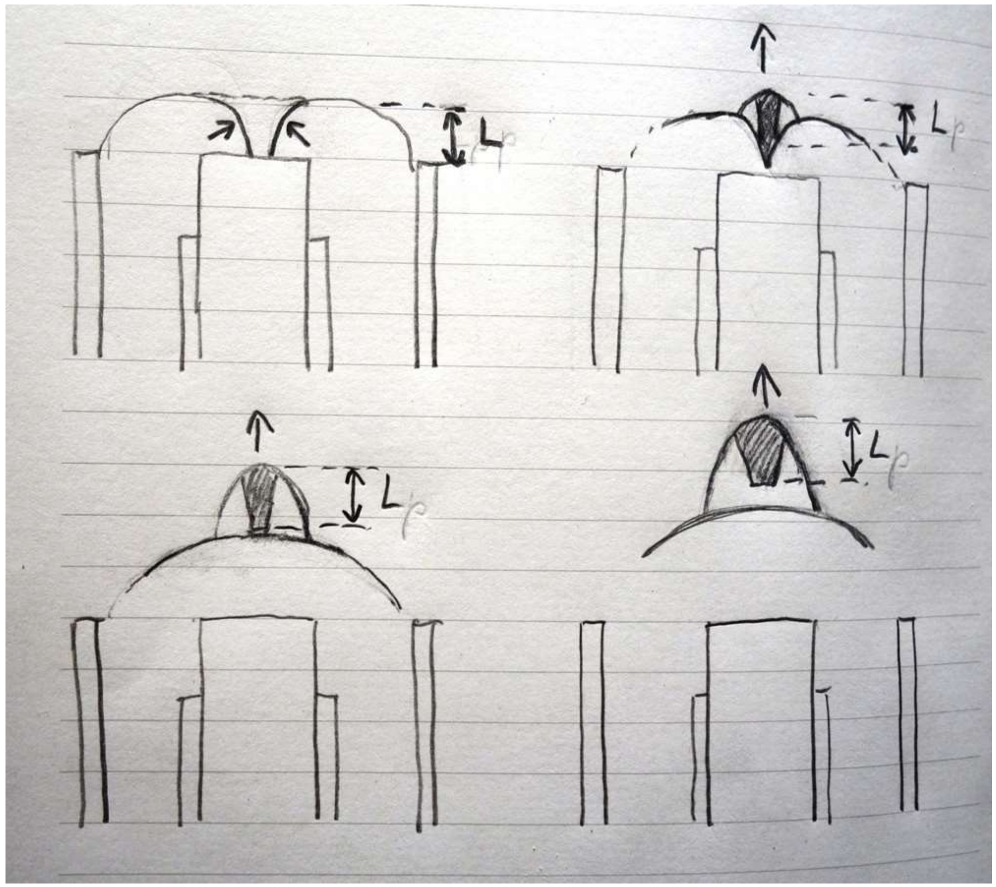
L
Lp
Lp
Lp

Plasma bursts after the pinch

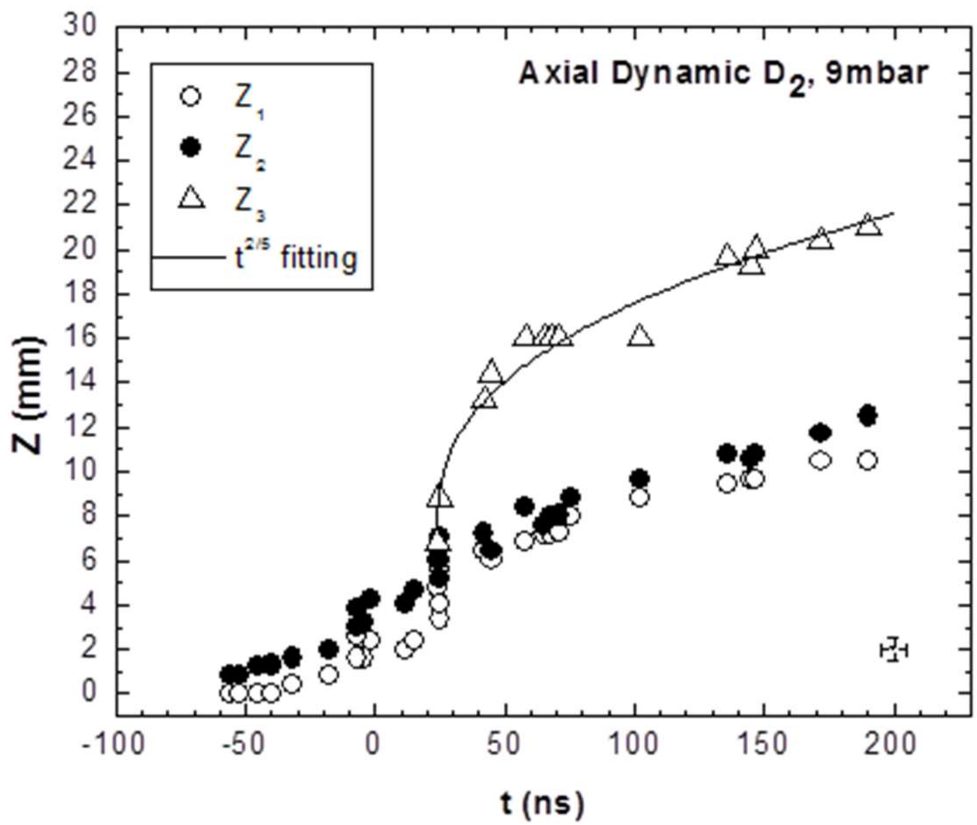

$$Z_3(t) - Z_3(t_0) = \left[\frac{75}{16\pi}\frac{(\gamma-1)(1+\gamma)^2}{(3\gamma-1)}\frac{E}{\rho_0}\right]^{\frac{1}{5}}(t-t_0)^{2/5}$$

L. Soto, C. Pavez, J. Moreno, M. J. Inestrosa, F. Veloso, G. Gutierrez, J. Vergara, F. Castillo, A. Clausse, H. Bruzzone and L. Delgado-Aparicio, Physics of Plasmas 21, 122703 (2014)

Damage Factor produced by Plasma bursts after the pinch

Total mass inside the bubble, m: ~ total pinch mass

(the pinch is ejected trough Z2, creating so the bubble)

The pinch density was previously measured using pulsed interferometry, thus the total pinch mass is **m ~ 1.5×10^{-10} kg**

C. Pavez and L. Soto, Physica Scripta T131, 014030 (2008)

Length of the ejected mass: ~ pinch length, L = 5.6 mm

Time of interaction, $\tau \sim L / v$

Tunable Damage Factor

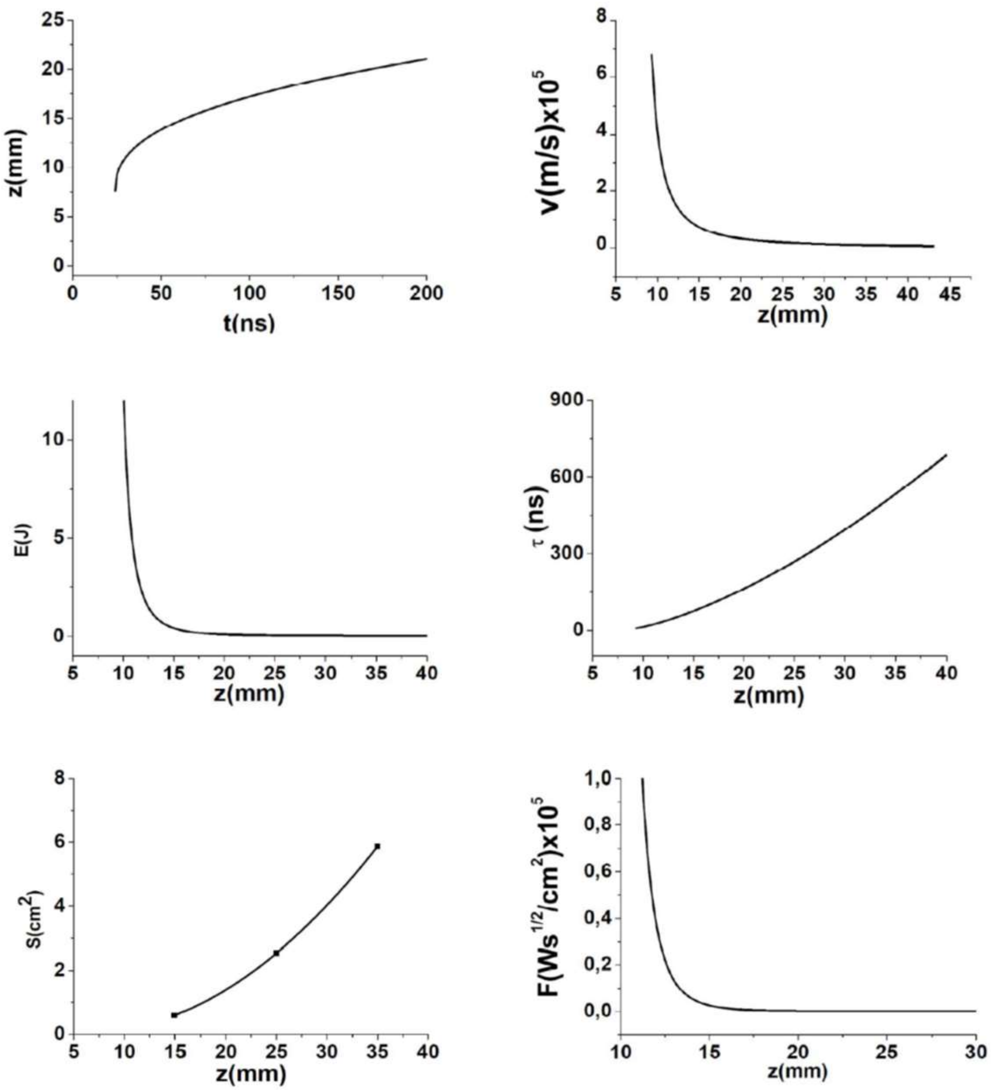

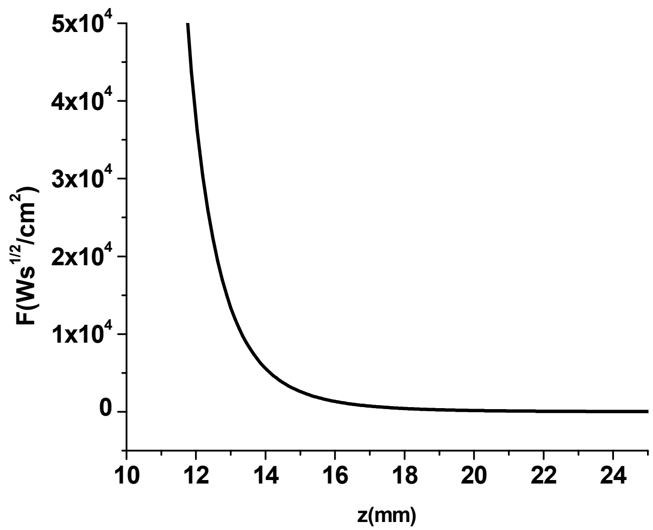

L. Soto et al, in preparation

Power flux density does not depend on PF energy

For PF devices:

$E/a^3 \sim$ const — a: anode radius — $n \sim$ const

$v \sim$ const

$T \sim$ const

$r_p \sim 0.1a$

$z_p \sim 0.8a$

Plasma ejected from the pinch (burst) on a target at Z, $\sim 1.5a < Z < 2.7a$

$m \sim m_p \; \alpha \; V_p \; \alpha \; a^3$

Thickness $\sim$ pinch length $L_p \; \alpha \; a$

Time of interaction $\tau = L / v \; \alpha \; a$

Cross section S: a^2

$$q \sim KE/\tau S \;\; \alpha \;\; m/\tau S \;\; \alpha \;\; a^3 / a\, a^2 \sim \text{const}$$

L. Soto et al, in preparation

6 order of magnitud in energy translates in only 1 order of magnitude in damage factor

damage factor, $F \sim q \cdot \tau^{1/2} \propto \tau^{1/2} \propto a^{1/2} \propto (E^{1/3})^{1/2}$

$$F \propto E^{1/6}$$

$a^3 \propto E$

PF, 1MJ	**F**
PF, 1kJ	**~ 1/3 F**
PF, 100J	**~ 1/5 F**
PF, 10J	**~ 1/7 F**
PF, 1J	**~ 1/10 F**

Roughly speaking

The damage factor for the PF-1000 (1MJ) at Poland is only 3.65 times greater than the damage factor for the PF- 400J (400J) at Chile.

L. Soto et al, in preparation

IOP Publishing | International Atomic Energy Agency Nuclear Fusion

Nucl. Fusion 55 (2015) 093011 (8pp) doi:10.1088/0029-5515/55/9/093011

Morphological and structural effects on tungsten targets produced by fusion plasma pulses from a table top plasma focus

M.J. Inestrosa-Izurieta[1,2], E. Ramos-Moore[3] and L. Soto[1,2]

[1] Comisión Chilena de Energía Nuclear, Casilla 188-D, Santiago, Chile
[2] Center for Research and Applications in Plasma Physics and Pulsed Power, P^4, Santiago-Curicó Chile
[3] Instituto de Física, Pontificia Universidad Católica de Chile, Santiago 7820436, Chile

E-mail: mj.inestrosa@cchen.cl and lsoto@cchen.cl

Received 30 January 2015, revised 17 June 2015
Accepted for publication 30 June 2015
Published 5 August 2015

CrossMark

PF400J: Fusion Plasma Pulses Source

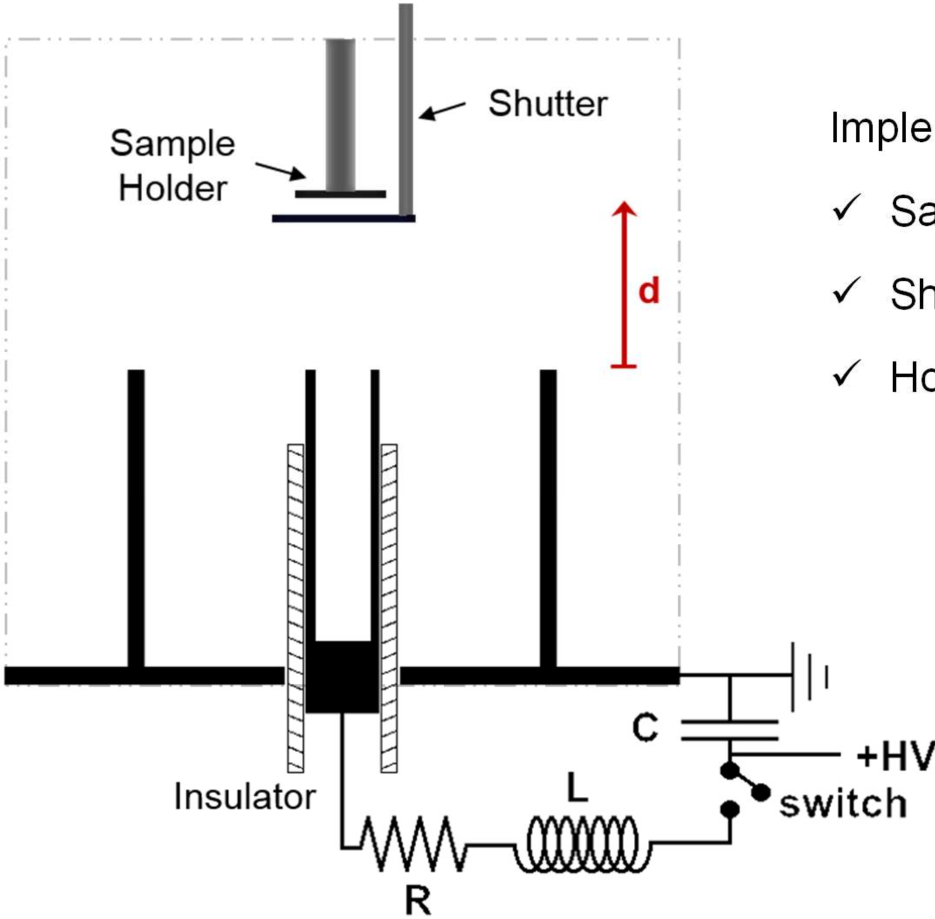

Implementation of:

- ✓ Sample holder ➡ avoiding ablation
- ✓ Shutter ➡ control exposure
- ✓ Hollow anode ➡ avoid anode material deposition

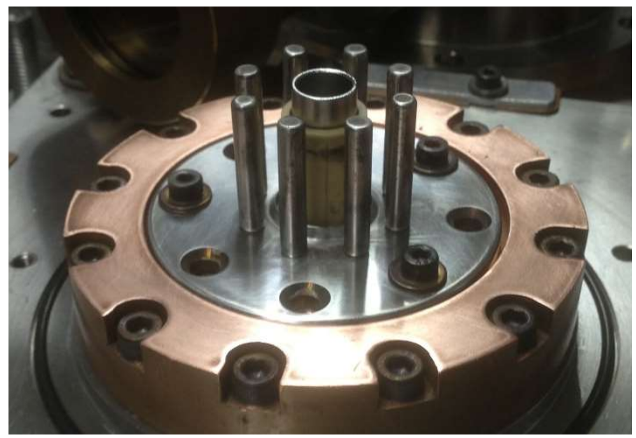

M. J. Inestrosa Izurieta, E. Ramos-Moore and L. Soto, Nuclear Fusion 55, 093011 (2015)

PF400J: Fusion Plasma Pulses Source
Tungsten target

$m \sim 1.5 \times 10^{-10}$ kg

L = 5.6 mm

$\tau \sim L / v$

Z (mm)	V (m/s)	S (cm²)	E/S (J/cm²)	τ (ns)	q (W/cm²)	$F = q\tau^{1/2}$ $(W/cm^2)s^{1/2}$
15	7.5×10^4	0.6	0.69	75	9.2×10^6	2.5×10^3
25	2.08×10^4	2.54	1.3×10^{-2}	270	4.7×10^4	24
35	1.05×10^4	5.87	1.4×10^{-3}	533	2.6×10^3	1.9

M. J. Inestrosa Izurieta, E. Ramos-Moore and L. Soto, Nuclear Fusion 55, 093011 (2015)

Morphological Effects on W
SEM

15 mm

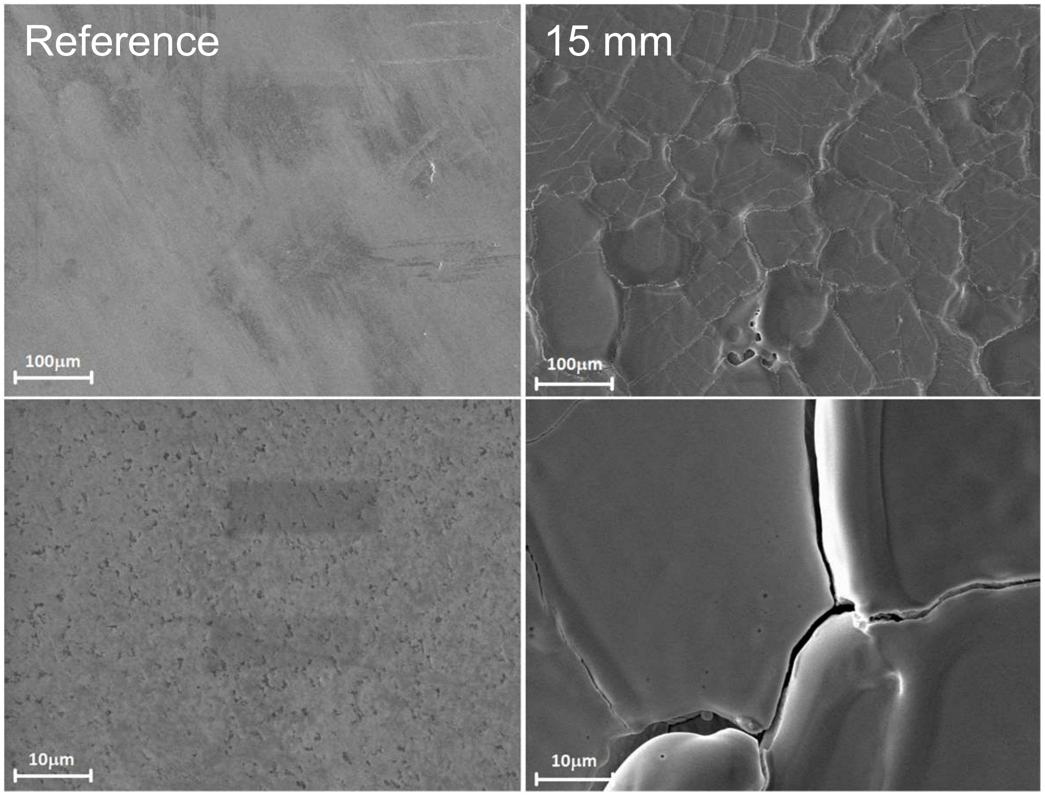

Scanning Electron Microscope images to comparison the extreme irradiation targets

- ✓ Ref. ➡ smooth surface
- ✓ 15 mm ➡ microcracks and holes surface melting
- ✓ 25 mm ➡ some melting
- ✓ 35 mm ➡ no melting

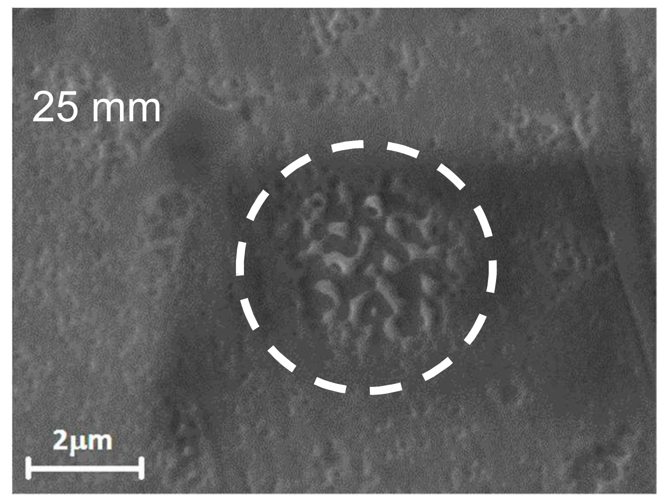

Scanning Electron Microscope image showing targets.

M. J. Inestrosa Izurieta, E. Ramos-Moore and L. Soto, Nuclear Fusion 55, 093011 (2015)

Studies of the plasma interacting with a target material on front of the anode using visible spectroscopy

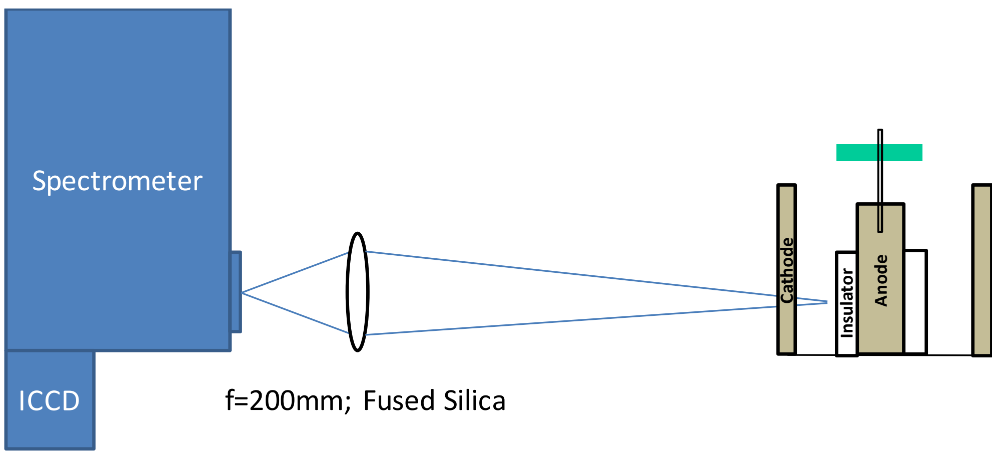

G. Avaria et al, in preparation

Discharge:

- Charging voltage ~27kV (~310 J)
- Frequency 0.06Hz (~ 16 s)

Diagnostics

- 0.5 m Cerny-Turner *Imaging* Spectrometer
  - 300 l/mm
  - Optical resolution (FWHM): 0.4 nm
- ICCD
  - FWHM: 3 ns

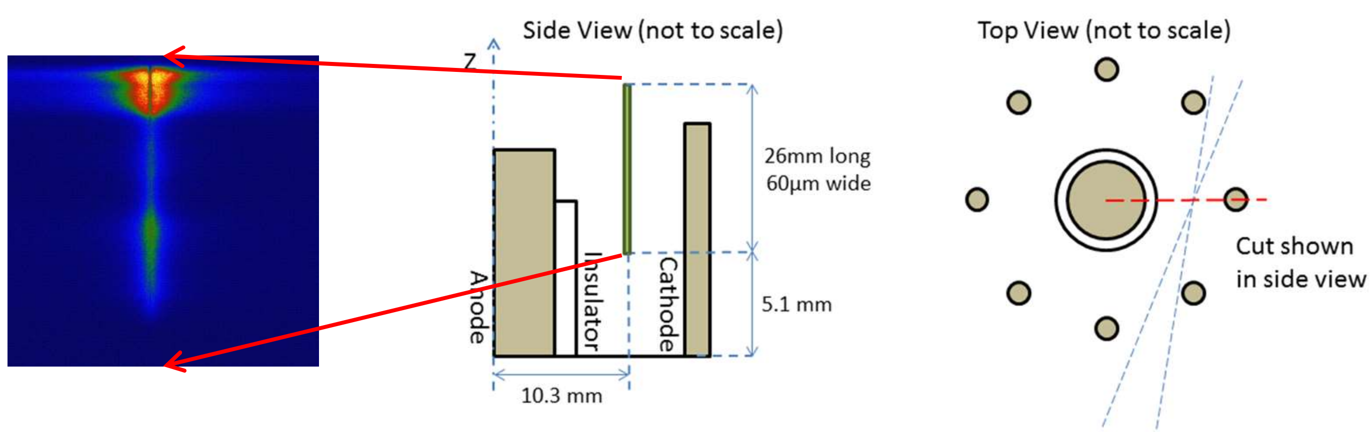

Studies of the plasma interacting with a target material on front of the anode using visible spectroscopy

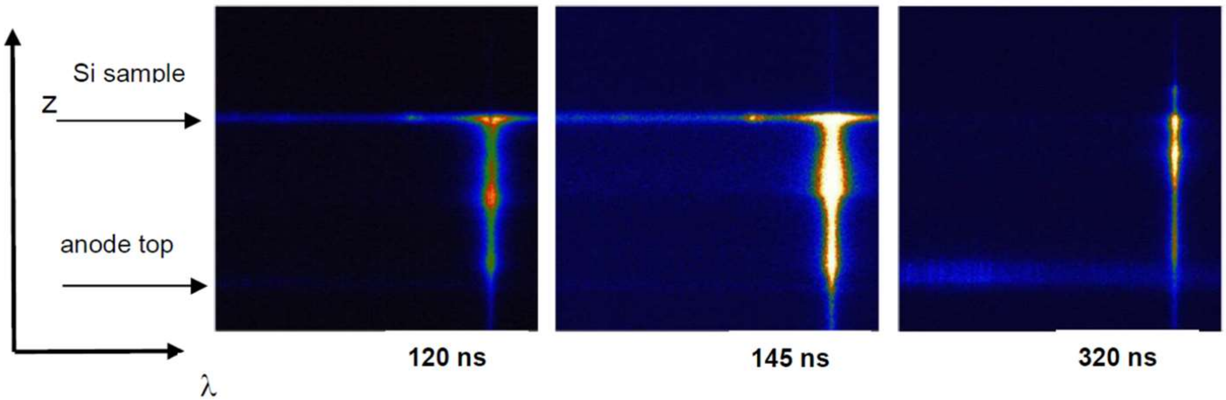

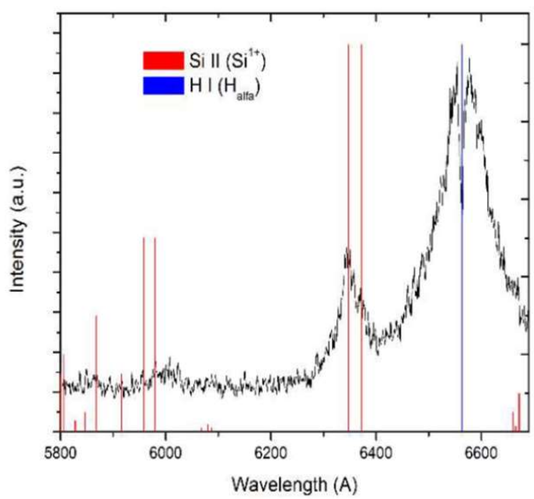

Visible spectra at different times for the region between the anode and the sample Si wafer, z axis is the axial position between the anode top and the sample, x axis is the wavelength λ. At 120 ns after the pinch Si II (Si^{1+}) is observed in the sample region. Also, the Hα emission is observed from the anode towards the sample. The spectrum close to the sample is shown at left. A Si and hydrogen plasma can be identified at the sample and a hydrogen-only plasma at the anode top. At 145 ns there is a similar emission as seen at 120 ns, but with more dense hydrogen plasma at the sample (inferred from the Hα line broadening) and hydrogen plasma at middle position between the anode top and sample. At 320 ns on the anode region Fe III (Fe^{2+}), Al II (Al^{1+}), Al III (Al^{2+}), O II (O^{1+}) can be identified. Si II is not observed on the sample region at that time. In addition, a plasma beyond the sample is observed.

G. Avaria et al, in preparation

Repetitive table top plasma focus to reproduce an equivalent damage on materials than the expected by type I ELMs in ITER

C (µF)	12
L (nH)	50
V (kV)	8.2
E (J)	403
I (kA)	127
T/4 (µs)	1,2
Anode radius (mm)	6
Anode lenght (mm)	60
Maximum repetition rate (Hz)	1

A tabletop PF devices to study the effects of thermonuclear plasmas on materials

L. Soto
Plasma Physics and Nuclear Fusion Laboratory
Chilean Nuclear Energy Commission

Repetitive table top plasma focus to reproduce an equivalent damage on materials than the expected by type I ELMs in ITER

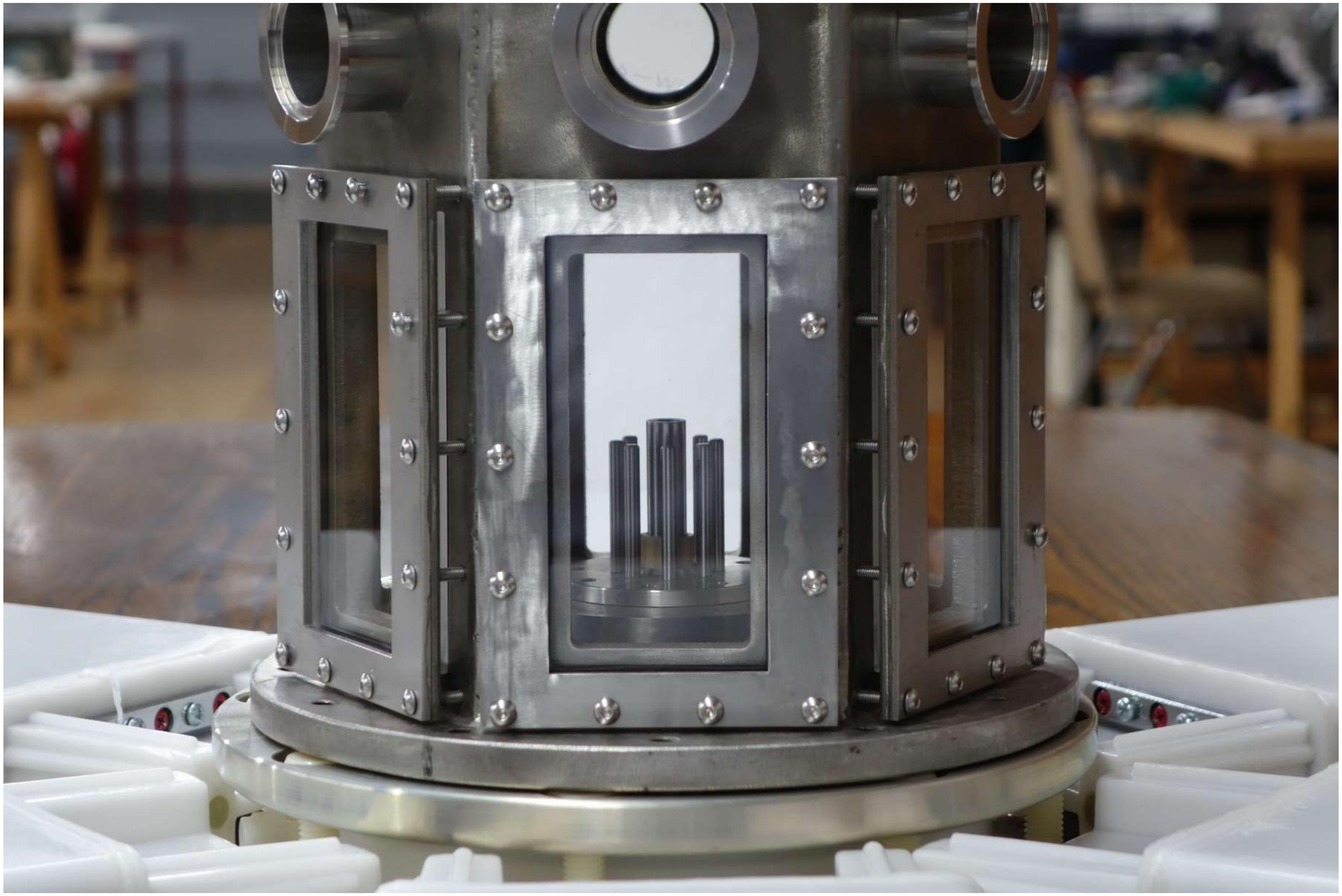

L. Soto
Plasma Physics and Nuclear Fusion Laboratory
Chilean Nuclear Energy Commission

Film deposition

AIP ADVANCES **7**, 105026 (2017)

Ti film deposition process of a plasma focus: Study by an experimental design

M. J. Inestrosa-Izurieta,[1,2,3,a] J. Moreno,[1,2,3] S. Davis,[1,2,3] and L. Soto[1,2,3]

[1] *Comisión Chilena de Energía Nuclear, Casilla 188-D, Santiago, Chile*

[2] *Center for Research and Applications in Plasma Physics and Pulsed Power, P^4, Santiago-Curicó, Chile*

[3] *Universidad Andres Bello, Departamento de Ciencias Fisicas, Facultad de Ciencias Exactas, Republica 220, Santiago, Chile*

(Received 27 July 2017; accepted 24 October 2017; published online 31 October 2017)

Film deposition

A study varying: **Voltage [kV] / Pressure [mbar] / Distance [mm] / # Pulses**

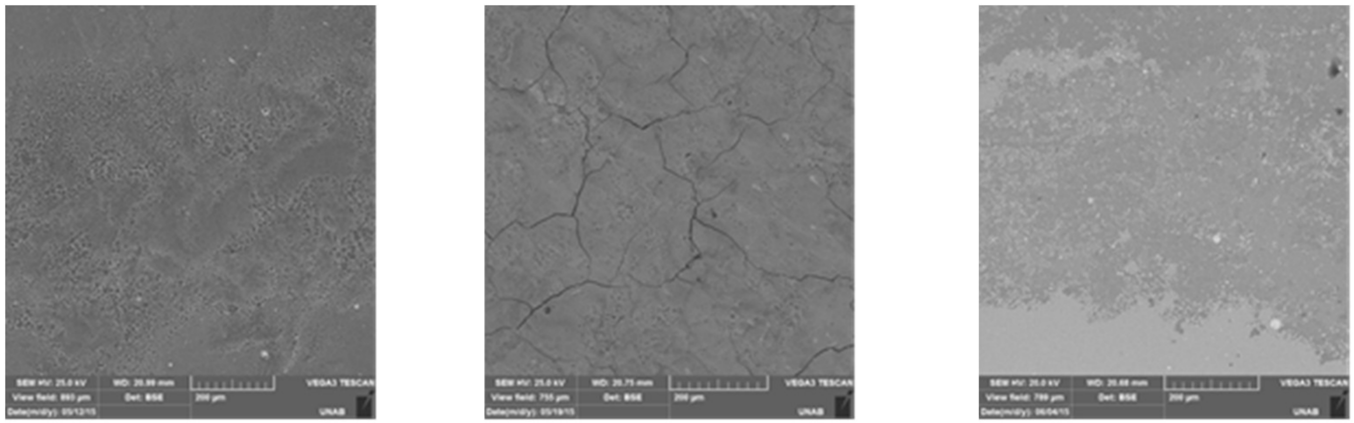

SEM images of selected Ti samples with marker length of 200µm on all the micrographs. From left to right 28/7/21/20, 27/6/9/50 and 27/6/15/80.

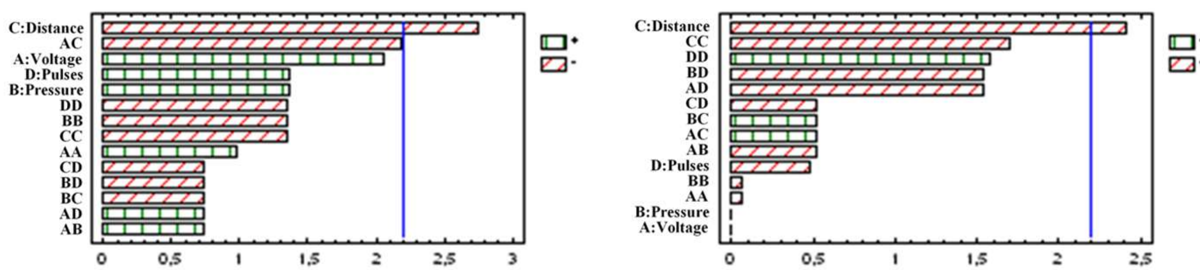

Standardized effects of Pareto chart for $TiSi_2$ (left) and Ti_5Si_3 (rigth) formation.

Inestrosa-Izurieta, J. Moreno, S. Davis and L. Soto, AIP Advances 7, 105026 (2017)

Applications to biology and biomedicine

Effects of pulsed radiation in cell

AIP ADVANCES 7, 085121 (2017)

CrossMark

Hundred joules plasma focus device as a potential pulsed source for *in vitro* cancer cell irradiation

J. Jain,[1,2] J. Moreno,[2,3,6] R. Andaur,[4] R. Armisen,[5,7] D. Morales,[2] K. Marcelain,[4,a] G. Avaria,[2,3,6] B. Bora,[2,3,6] S. Davis,[2,3,6] C. Pavez,[2,3,6] and L. Soto,[2,3,6,a]

[1]*Universidad de Talca, 2 Norte 685, Casilla 721, Talca, Chile*
[2]*Comisión Chilena de Energía Nuclear, Casilla 188-D, Santiago, Chile*
[3]*Center for Research and Applications in Plasma Physics and Pulsed Power, Santiago 7600713, Santiago, Chile*
[4]*Departamento de Oncología Básico-clínica, Facultad de Medicina, Universidad de Chile, Independencia 1027, Independencia, Santiago, Chile*
[5]*Centro de Investigación y Tratamiento del Cáncer, Facultad de Medicina, Universidad de Chile, Independencia 1027, Independencia, Santiago, Chile*
[6]*Universidad Andres Bello, Departamento de Ciencias Fisicas, Republica 220, Santiago, Chile*
[7]*Current affiliation: Center for Excellence in Precision Medicine, Pfizer Chile, Santiago 7810305, Santiago, Chile*

(Received 6 May 2017; accepted 21 August 2017; published online 29 August 2017)

Mathematics is all that is not understood.

Physics is all that does not work.

Chemistry is everything that smells bad.

Biology is all that is green and that it crawls.

L. Soto
Plasma Physics and Nuclear Fusion Laboratory
Chilean Nuclear Energy Commission

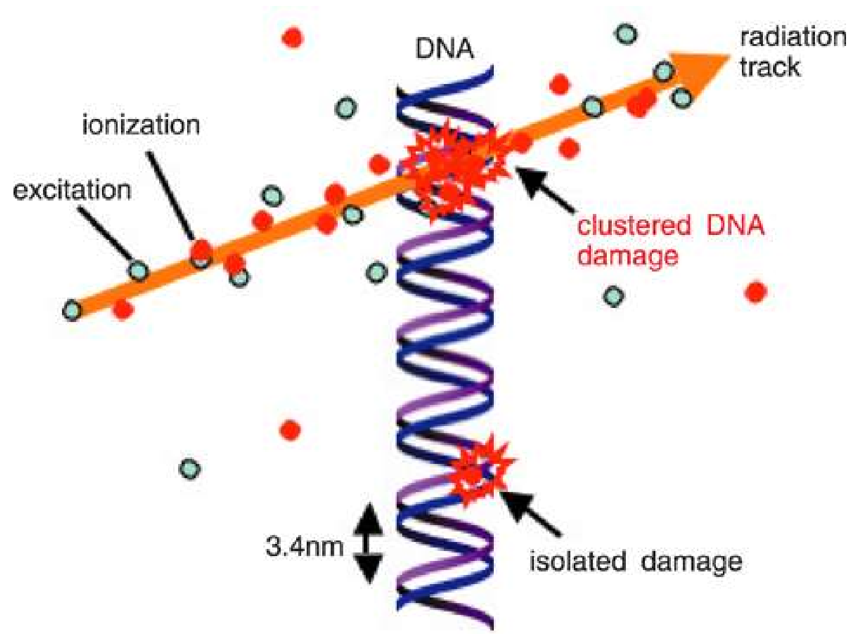

L. Soto
Plasma Physics and Nuclear Fusion Laboratory
Chilean Nuclear Energy Commission

Effects of pulsed radiation in cell

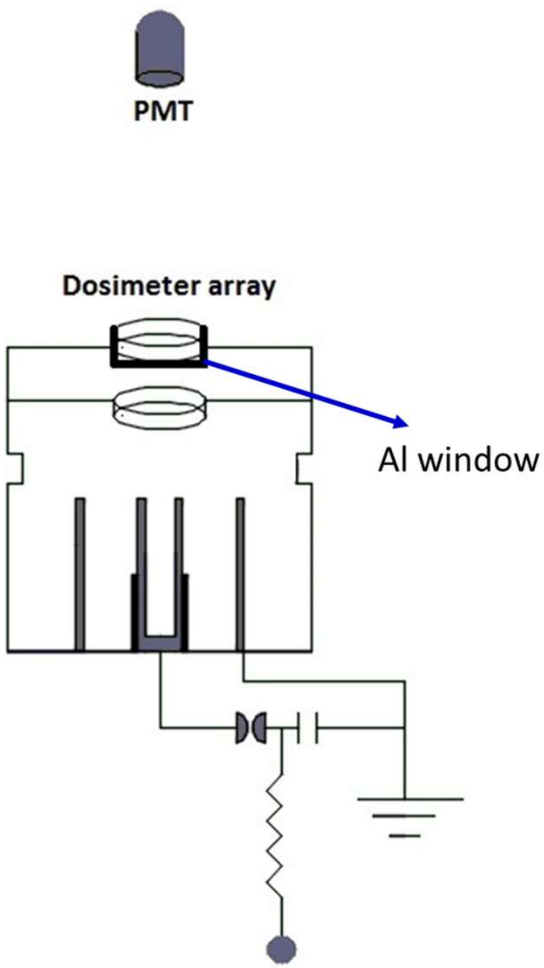

"J. Jain, J. Moreno, R. Andaur, R. Armisen, D. Morales, K. Marcelain, G. Avaria, B. Bora, S. Davis, C. Pavez, and L. Soto, AIP Advances **7**, 085121 (2017)

Effects of neutron and x-ray pulses on cancer cell

DNA damage DSB

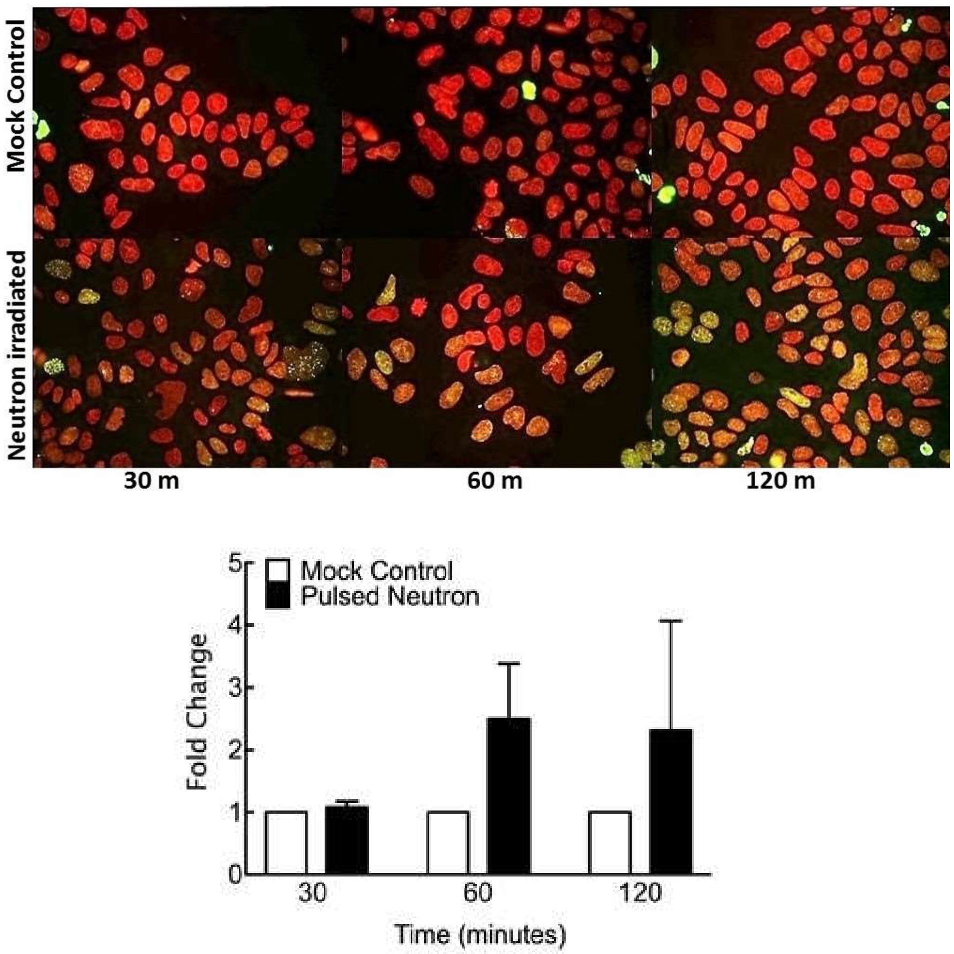

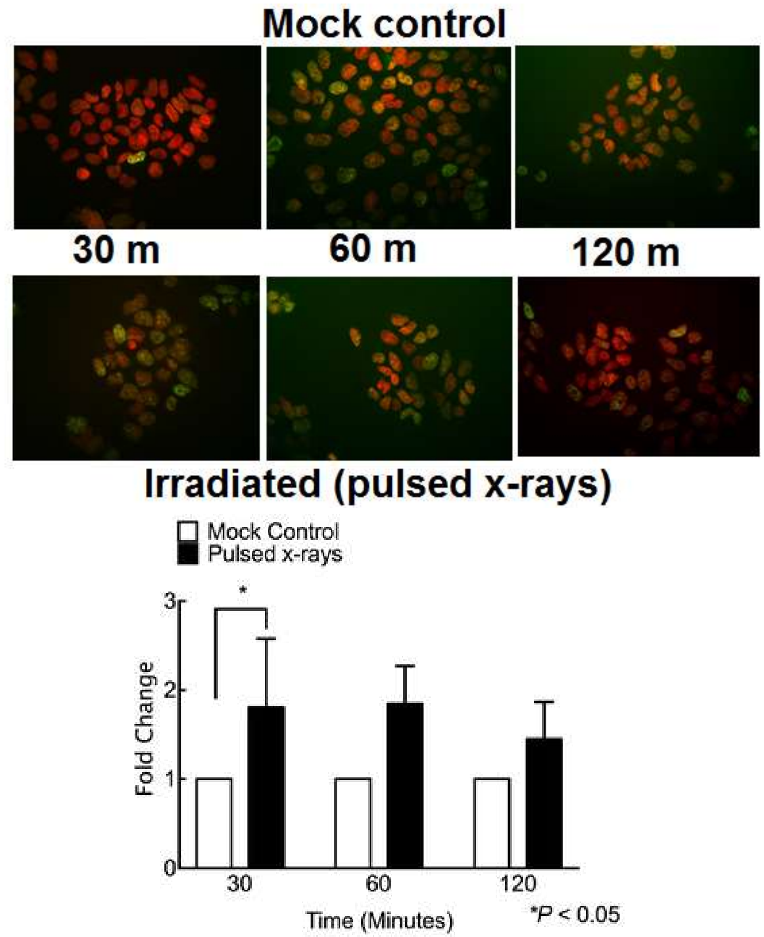

J. Jain, J. Moreno, R. Andaur, R. Armisen, D. Morales, K. Marcelain, G. Avaria, B. Bora, S. Davis, C. Pavez, and L. Soto, AIP Advances 7, 085121 (2017)

- Cell death was absent in case pulsed x-rays irradiation.
- Neutron irradiation provides cell death at ultralow doses but DNA damage with higher statistical insignificance.
- The effect depends on the repair time of the cells. Therefore, the time between pulses is a relevant parameter

Joint ICTP-IAEA Workshop on Dense Magnetized Plasma and Plasma Diagnostics, Triste, Italy, November 15-17, 2010

Jalaj Jain was a participant and after he made his PhD in Chile in our group in combination with biologist of University of Chile.

J. Jain, J. Moreno, R. Andaur, R. Armisen, D. Morales, K. Marcelain, G. Avaria, B. Bora, S. Davis, C. Pavez, and L. Soto, AIP Advances 7, 085121 (2017)

Pulsed Plasma Thruster for nanosatellites based on ultra-miniaturized Plasma Focus

Nanosatellite SUCHAI 2017
University of Chile

SUCHAI-1
10 cm x 10 cm x 10 cm
At present in orbit and in operation

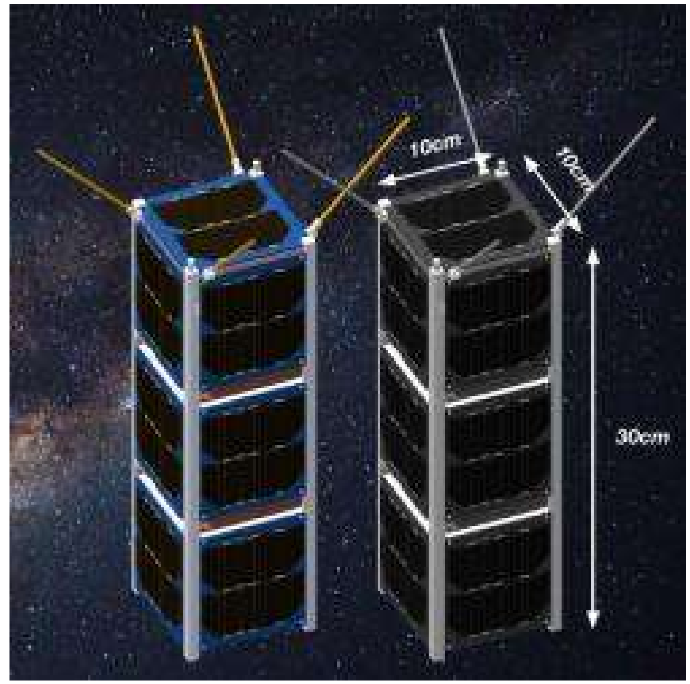

SUCHAI-2 and 3
At present under construction

M. Diaz *et al.*, Advances in Space Research, 58, 2134-2147 (2016)

Typical PPT diagram

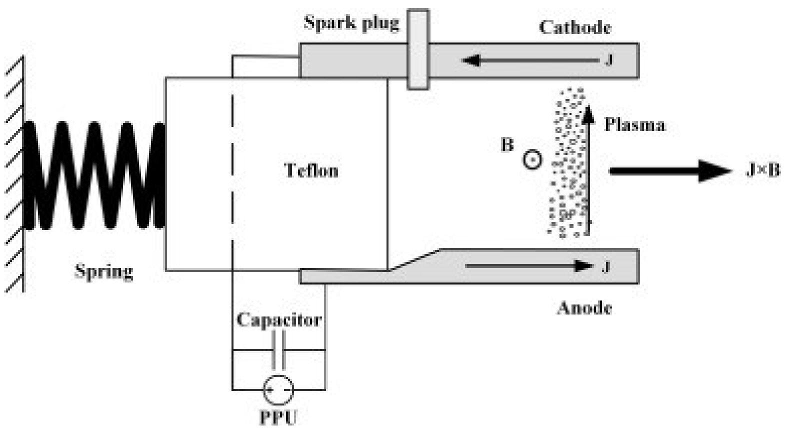

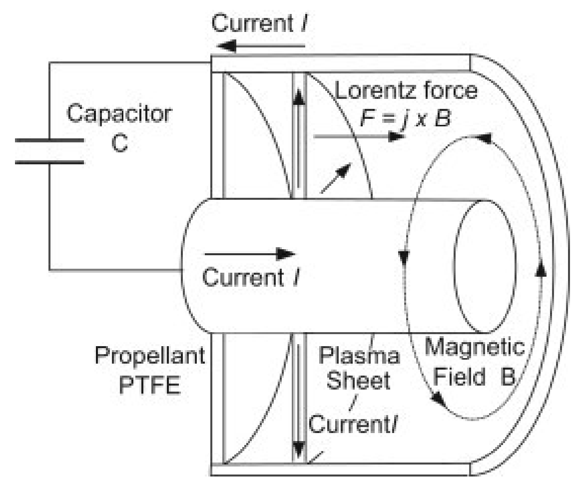

parallel plate electrodes

Coaxial electrodes

Thrust estimations from our previous work in PF devices

- On the one hand, to obtain an estimation for a miniature plasma thruster operating with an energy of the order of **1J**, based on plasma focus technology and its scaling laws, we can assume an ejected mass $\mathbf{m_e \sim 4 \times 10^{-13}}$ **kg** with a velocity $\mathbf{v_e \sim 5 \times 10^5}$ **m/s**. Thus, an impulse bit

  $\mathbf{I_{bit} = \Delta p = m_e\, v_e \sim 2 \times 10^{-7}}$ **Ns** is estimated.

  Considering that the mean propulsion force during a second as $\mathbf{\langle F \rangle = I_{bit}\, f}$, with f the operation frequency, the mean thrust could be **0.2, 2 and 20 μN** for an operation frequency of **1, 10 and 100 Hz** respectively.

- On the other hand, from electromagnetic estimation for a coaxial plasma gun (axial phase of a plasma focus), imposing the condition that the plasma reaches the end of the electrodes coincident with maximum current, i.e. at a time of quarter of period of the discharge,

  $\mathbf{\Delta p = F_{mag}\,(\tau/4) = (\mu_0/4)\, I^2 \ln(b/a)\, (LC)^{1/2}}$, with I the peak current, C de capacitance of the capacitor, L the total inductance, a anode radius and b cathode radius. Using $I = V\,(C/L)^{1/2}$,

  $\mathbf{\Delta p = (\mu_0/4)\, V^2 \ln(b/a)\, C^{3/2}\, L^{-1/2}}$.

  For a device with a capacitor of 225nF charging at 3kV an energy stored of 1J is achieved. Assuming a=0.5mm and b=1.25mm, and 5nH of inductance (that is possible achieved in compact devices, like Nanofocus designed and built at CCHEN a value for $\mathbf{\Delta p \sim 3.8 \times 10^{-6}}$ **Ns** is obtained. Thus, with **1, 10 and 100 Hz**, the mean thrust could be **3.8, 38 and 380 μN** respectively.

  Both estimations are consistent with the literature for orientation systems for CubeSats, and are enough to support our hypothesis and encourage to pursue a research project.

L. Soto
Plasma Physics and Nuclear Fusion Laboratory
Chilean Nuclear Energy Commission

Experiements on PPT in modified Nanofocus

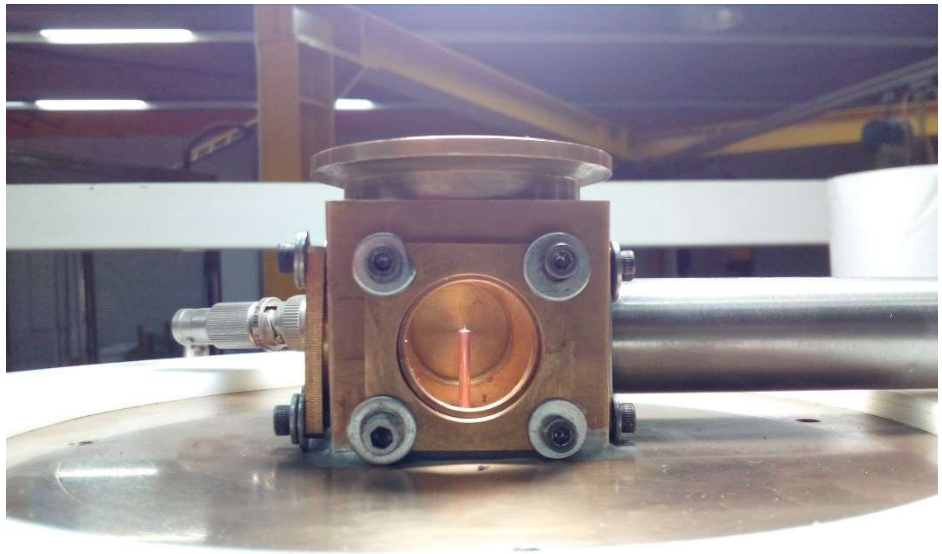

Electrodes
R_{ci}: 1.1 mm, R_{ce}: 0.85 mm
R_a : 0.35 mm

Modified Nanofocus with PPT electrodes
p ~ 10^{-4} mbar

"Pulsed Plasma Thruster Based On Ultra-miniaturized Plasma Focus" L. Soto, J. Pedreros, R. Silva, P. Maldonado, G. Avaria, C. Pavez, J. Moreno, and M. Diaz, 19th International Congress on Plasma Physics, ICPP 2018, Vancouver, Canada, June 2018.

Experiments on PPT in modified Nanofocus

A) Coaxial plasma gun with cathode and anode extended (as in figure 1b)

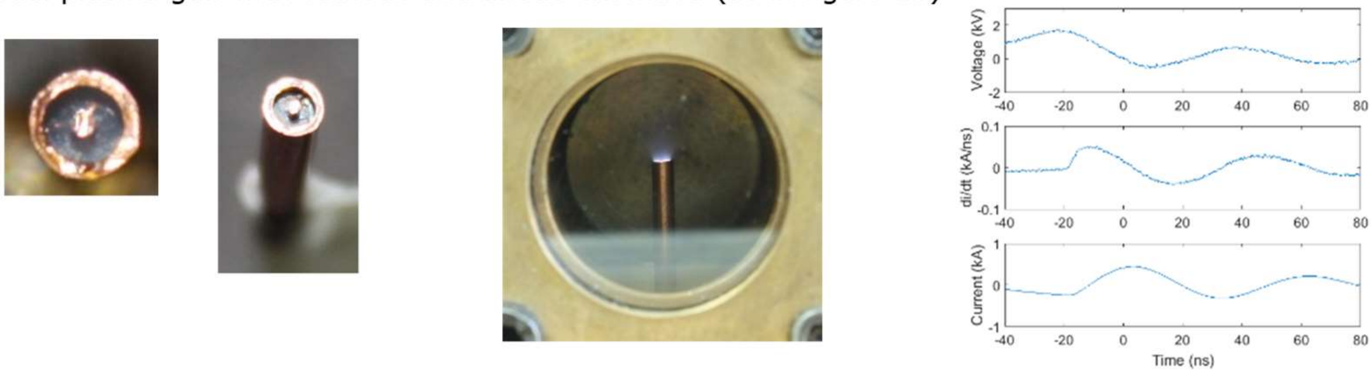

Left: Photograph of plasma gun. Center: plasma discharge. Right: voltage, current derivative and current signals. Voltage breakdown 1.75±0.2 kV.

B) Coaxial plasma gun with cathode extended

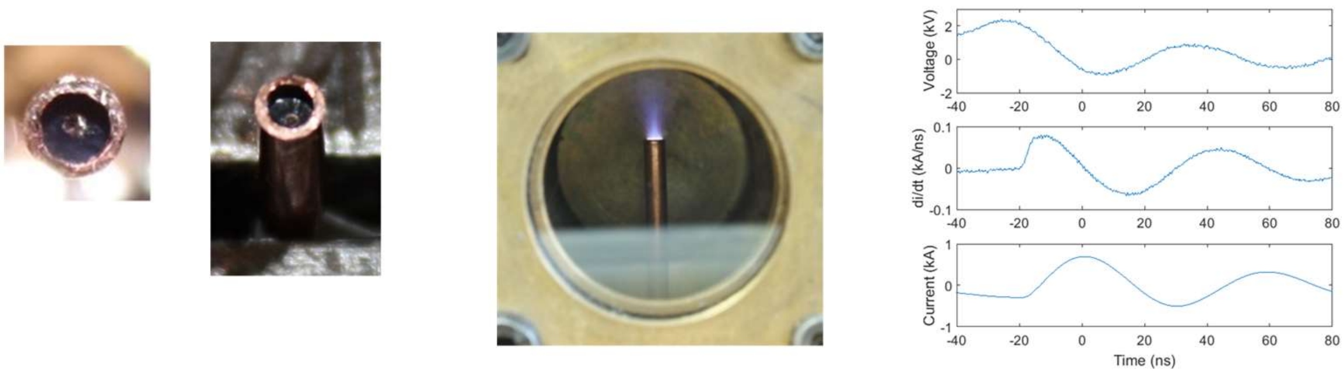

Left: Photograph of plasma gun. Center: plasma discharge. Right: voltage, current derivative and current signals. Voltage breakdown 2.2±0.1 kV.

"Pulsed Plasma Thruster Based On Ultra-miniaturized Plasma Focus" L. Soto, J. Pedreros, R. Silva, P. Maldonado, G. Avaria, C. Pavez, J. Moreno, and M. Diaz, 19th International Congress on Plasma Physics, ICPP 2018, Vancouver, Canada, June 2018.

Next Lecture

How to build a small Plasma Focus
Recipes and tricks

L. Soto
Plasma Physics and Nuclear Fusion Laboratory
Chilean Nuclear Energy Commission